Aspects topologiques des flots en dimension 3

—

Topological aspects of flows on 3 dimensions

Ana Rechtman

3 novembre 2017

Para Ema, como todo.

Remerciements

Il y a à peu près 10 ans j'ai commencé à faire des mathématiques ; remercier tous ceux que j'ai rencontrés, ceux qui m'ont aidé en écrivant des lettres de recommandation, ceux que j'ai écouté faire des exposés motivants, ceux qui m'ont raconté leurs idées, ceux qui ont fait un petit commentaire crucial sur ma recherche ou posé la question à laquelle j'aurais dû penser avant, me semble aujourd'hui impossible. Je sais que je vais sûrement oublier quelqu'un, mais je vous remercie tous. Je vais ici me restreindre, sans comprendre très bien les limites.

Je dois commencer par Pierre. Merci de savoir me suivre par moments et de me forcer à aller au-delà de mes peurs d'autrefois. C'est comme ça que nous avons fait trois déménagements transatlantiques ensemble et fait d'une longue liste d'appartements notre *hogar*. Merci aussi d'être toujours critique sur mes décisions professionelles, même si des fois je ne fais pas attention à tes opinions.

Une bonne partie de ce mémoire est dédiée aux résultats que j'ai obtenus avec Steve Hurder, une collaboration qui va bien au-delà du cadre strictement professionel. Merci Steve pour l'accueil à Chicago, pour les après-midi d'hiver devant la cheminée chez toi, mais surtout merci de t'être engagé si fortement dans un projet qui semblait innocent il y a 8 ans, et que nous n'avons pas encore fini.

Le reste de ce mémoire est dédié à des résultats obtenus en collaboration avec Pierre Dehornoy. Merci Pierre de m'aprendre de belles mathématiques et merci pour un projet de recherche qui ne fait que commencer. Je te remercie aussi beaucoup d'avoir changé la date de la conférence à Moscou de janvier à avril, le voyage Mexico-Moscou en janvier aurait été très difficile pour moi.

Même si à ce jour nous ne sommes pas encore arrivés à écrire quelque chose ensemble, je veux remercier Alberto Verjovsky, pour toutes les heures sous son arbre à discuter. Je tiens également à remercier tous mes collaborateurs, tant ceux avec qui j'ai réussi à publier quelque chose, comme ceux avec qui nous avons compris que nos idées ne marchaient pas, ou ceux avec qui j'ai toujours l'espoir de résoudre un petit problème.

Je tiens à remercier Nalini Anantharaman d'avoir accepté d'être garante de cette habilitation, même si je lui ai demandé au dernier moment. Un grand merci à Amie Wilkinson, Christian Bonatti et Daniel Peralta Salas pour avoir accepté de rapporter sur mon mémoire. Je remercie aussi Christophe Bavard, Frédéric Le Roux et Étienne Ghys de faire partie du jury de mon habilitation.

Je dois dire que j'ai toujours bénéficié de conditions de travail exceptionnelles, je veux remercier les équipes administratives et tous les collègues des laboratoires où j'ai été.

Ce mémoire a été écrit au Mexique, où je travaille actuellement. Je tiens à remercier Yann Bugeaud, Thomas Delzant, Delphine Karleskind, Jessica Maurer-Spoerk, Géraldine Schverer et Grégory Thureau pour leur aide pour réaliser les démarches bureaucratiques à distance et pour leurs explications des étapes à franchir pour arriver à la soutenance.

Une force incroyable a détruit une petite partie de ma ville il y a quelques semaines. 32 ans avant (comptés jour pour jour) cette force avait détruit une grande partie de la même ville. Cette

fois elle m'a laissé sans maison et j'ai mis les dernières semaines à recréer une routine que j'apprécie plus que jamais. Heureusement, ce mémoire était déjà écrit, mais il me rappelera toujours les 19 septembre 2017 et 1985.

Mexico, 24 octobre 2017.

Contents

List of Figures

Travaux de recherche

Je présente ici mes travaux de recherche, dans l'ordre chronologique. Je commence avec les deux papiers qui présentent les résultats de ma thèse.

(P1) **Existence of periodic orbits for geodesible vector fields on closed 3-manifolds.** Ergodic Theory and Dynamical Systems 30, no. 6, 1817 - 1841, 2010.

(P2) **Minimal Følner foliations are amenable.** En collaboration avec Fernando Alcalde Cuesta. Discrete and Continuous Dynamical Systems - Series A, Vol. 31, no. 3, 2011.

Le papier (P1) correspond à la première partie de ma thèse dédiée à la question de l'existence d'orbites périodiques pour les flots géodésibles. J'ai montré leur existence sous certaines hypothèses supplémentaires. Dans les preuves, j'utilise la technique des courbes pseudoholomorphes due à Hofer [Hof93]. Après ma thèse, Klaus Niederkrüger et moi avons utilisé cette technique pour montrer l'existence d'orbites périodiques pour les flots de Reeb en dimension plus grande que 3, en la présence de sous-variétés feuilletées par la structure de contact. Le résultat fait l'objet du papier :

(P3) **The Weinstein conjecture in the presence of submanifolds having a Legendrian foliation.** En collaboration avec Klaus Niederkrüger. Journal of Topology and Analysis, Volume 3, Issue 4, 405-421, 2011.

Le papier (P2) correspond à la deuxième (et dernière) partie de ma thèse, il s'agit d'étudier deux propiétés de moyennabilité pour des feuilletages (ou pour les pseudogroupes). Une condition est locale (c'est la condition dite de Følner) et l'autre est globale. Mes résultats on été améliorés lors de ma collaboration avec Fernando Alcalde Cuesta. Nous avons écrit un deuxième papier ensemble :

(P4) **Averaging sequences.** En collaboration avec Fernando Alcalde Cuesta. Pacific Journal of Mathematics, Vol. 255, No. 1, 1-23, 2012.

Voici la liste de mes autres travaux :

(P5) **The dynamics of generic Kuperberg flows.** En collaboration avec Steve Hurder. Astérisque, Vol. 377, 1-250, 2016.

(P6) **Two proofs of Taubes' theorem on strictly ergodic flows.** En collaboration avec Victor Kleptsyn. À paraître dans les mémoires de la conférence *II Reunión de Matemáticos Mexicanos en el Mundo (MMM2014).*

(P7) **Aperiodicity at the boundary of chaos.** En collaboration avec Steve Hurder. À paraître dans Ergodic Theory and Dynamical Systems.

(P8) **Equivalence of Deterministic walks on regular lattices on the plane.** En collaboration avec Raúl Rechtman. Physica A, Vol. 466, 69 - 78, 2017.

(P9) **The trunkenness of a volume-preserving vector field.** En collaboration avec Pierre Dehornoy. À paraître dans Nonlinearity.

(P10) **Perspectives on Kuperberg flows.** En collaboration avec Steve Hurder. À paraître dans les mémoires de la conférence *31st Summer Conference on Topology and its Applications*.

Dans ce texte je présente des résultats tirés des papiers (P5), (P7) et (P9). Le papier (P10) est une compilation de questions autour des flots de Kuperberg, il est cité dans ce texte.

Je vais donc utiliser quelques lignes pour vous raconter les résultats des articles (P6) et (P8), avant d'introduire mon mémoire. Dans (P6) nous avons trouvé deux preuves alternatives de l'énoncé suivant, qui a été originalement prouvé par C. H. Taubes [Tau09] en utilisant des invariants de Seiberg-Witten. Nous disons qu'un champ de vecteurs est *strictement ergodique* si son flot admet une unique mesure invariante et si cette mesure est un volume.

THÉORÈME. *Soit X un champ de vecteurs sur $\mathbb{S}^3$ strictement ergodique. Alors l'hélicité de X est nulle.*

L'hélicité est définie dans la Section 2.1, il s'agit d'un invariant de conjugaison C^1 pour les flots qui préservent un volume.

Dans l'article (P8) nous établissons une équivalence entre deux modèles discrets de propagation de gaz dans un réseaux, appelés en anglais *Lorenz lattice gases*. Ils ont des propriétés remarquables. Notre papier donne une recette pour passer d'un modèle à un autre sur des réseaux réguliers du plan.

Tous mes papiers peuvent être consultés sur ma page web :

`www.matem.unam.mx/rechtman/publications.html`

Introduction

Dans ce mémoire je présente des résultats reliés à l'étude des flots en dimension 3. Le mémoire est divisé en deux chapitres. Le premier est dédié à mon travail pour comprendre l'ensemble minimal du piège de Kuperberg, ou dit d'une autre façon, l'ensemble minimal des seuls exemples connus de flots lisses sans points fixes et sans orbites périodiques sur $\mathbb{S}^3$. Dans le second, j'explique comment construire une quantité appelée *tronc* associée à un flot sur $\mathbb{S}^3$ muni d'une mesure invariante, qui est préservée par conjugaison topologique. Ce résultat s'inscrit dans la démarche consistant à trouver des invariants pour les flots provenant d'invariants pour les nœuds.

Les résultats présentés dans le premier chapitre ont été obtenus en collaboration avec Steve Hurder, avec qui j'ai commencé à collaborer lors de mon postdoctorat à Chicago. Nous nous sommes donné pour tâche de comprendre l'ensemble minimal du piège de Kuperberg. La première observation importante pour ce faire est que la construction dépend de certains choix, je cite É. Ghys [Ghys95] :

> *Par ailleurs, on peut construire beaucoup de pièges de Kuperberg et il n'est pas clair qu'ils aient la même dynamique.*

Les choix donnent toujours un piège dont le flot est C^∞, sans orbites périodiques et avec un unique ensemble minimal, mais nous ne savons pas si l'ensemble minimal est le même pour tous les choix possibles. En effet, une question qui reste ouverte est de savoir s'il y a des choix pour lesquels l'ensemble minimal est de dimension 1. Dans notre travail, nous imposons des hypothèses supplémentaires à la construction du piège qui nous permettent de montrer que l'ensemble minimal est de dimension topologique 2 et d'en déduire d'autres propiétés dynamiques du flot. Nous appelons ces choix *génériques*, car il s'agit de demander que deux propiétés de la construction soient de nature quadratique. Nous appelons les flots obtenus des *flots de Kuperberg génériques*. Je présente ces hypothèses brièvement dans la remarque 1.2.1 et avec plus de détails dans la section 1.6.

Il faut mentionner que dans la catégorie des flots linéaires par morceaux, Greg et Krystyna Kuperberg parviennent à construire un piège de Kuperberg dont l'ensemble minimal est de dimension 1 [KK96]. Aussi, si un piège de Kuperberg est tel que son ensemble minimal est de dimension 1, l'ensemble minimal est contenu dans un esemble invariant de dimension topologique 2 qui a la même structure que l'ensemble minimal du cas générique.

Comment étudier un ensemble minimal ? Quels sont les aspects importants ?

Une première approche est de se faire une image de cet ensemble minimal, de le visualiser. Finalement c'est un ensemble plongé dans $\mathbb{R}^3$ et 3 est encore une petite dimension. J'ai essayé dans ce mémoire d'expliquer l'image que nous nous sommes faite de cet ensemble, la section 1.3 donne une façon de comprendre comment il est structuré. Tout n'y est pas dit, j'ai décidé de ne pas rentrer dans certaines complications et détails. Il s'agit donc d'une image idéalisée de l'ensemble, qui permet de comprendre les autres aspects que nous avons décidé d'étudier.

Une seconde approche naturelle est la *théorie de la forme*. Introduite par Borsuk [Bor68], elle permet d'étudier certains aspects des ensembles plongés dans un espace euclidien, en étudiant des

suites de voisinages de plus en plus petits. Nous avons été guidés par une question de K. Kuperberg : est ce que la forme de l'ensemble minimal est stable ? Comme expliqué dans la section 1.4.1, nous savons que la réponse à cette question est négative (dans le cas d'un flot de Kuperberg générique). Le concept d'ensemble «movable» est un autre concept important dans la théorie de la forme. Nous ignorons si l'ensemble minimal des flots de Kuperberg génériques est «movable». Je conjecture que oui.

Nous comprenons donc comment visualiser cet ensemble minimal exceptionnel (c'est-à-dire transversement un ensemble de Cantor) de dimension topologique 2. Il est, par minimalité, localement homogène, mais il n'est pas globalement homogène. Comme expliqué dans le théorème 1.3.5, l'ensemble ne forme pas une lamination, mais il contient un ouvert dense de dimension 2 qui est une lamination $\mathcal{L}$ avec des feuilles ouvertes. Nous pouvons donc considérer la dynamique de cette lamination et la comparer à la dynamique du flot restreint à l'ensemble minimal.

Cet approche nous a permis de construire des pseudogroupes agissant, soit dans un rectangle presque transverse au flot, soit dans une transversale à la lamination $\mathcal{L}$. Il s'agit, par leur nature et par la construction, de pseudogroupes différents mais semblables, avec des ensembles de générateurs similaires. Le premier de ces pseudogroupes est décrit brièvement dans la section 1.4. En utilisant la notion d'entropie pour les pseudogroupes, introduite par Ghys, Langevin et Walczak [GLW88], nous avons étudié ces pseudogroupes. Dans la section 1.4.2, j'explique quelques-uns des résultat obtenus.

Les pseudogroupes utilisés dans [P5] ont tous la propiété que le nombre de points séparés par des mots de longueur n (avec un ensemble de générateurs fixé) croît comme l'exponentielle de n^α, pour un certain $\alpha \in (0, 1)$. Ils sont donc tous d'entropie nulle, mais d'entropie *lente* positive (les définitions sont données dans la section 1.4.2). Cette affirmation s'étend au flot restreint à l'ensemble minimal : le flot est d'entropie topologique nulle, mais a une entropie lente positive. Le fait que l'entropie topologique du flot soit nulle est aussi une conséquence d'un théorème de Katok [Kat80], comme remarqué par É. Ghys [Ghys95].

Avec l'objectif de trouver des flots à entropie topologique positive près des flots de Kuperberg, nous avons étudié des déformations de la construction du piège dans [P7]. Nous avons alors trouvé une famille C^∞ à un paramètre contenant un flot de Kuperberg et des flots à entropie positive. La construction et quelques idées des preuves forment le contenu de la section 1.5.

Le flot de Kuperberg est donc une bifurcation dans l'espace des flots sur une variété fermée de dimension 3. Il s'agit d'une situation non générique, mais ce flot doit probablement être entouré d'autres bifurcations parmi lesquelles il pourrait y avoir des bifurcations génériques. Je ne sais pas, pour le moment, si l'étude d'un voisinage du piège parmi les bifurcations est abordable.

Par ailleurs, les pièges à entropie topologique positive construites dans [P7] contiennent une famille dénombrable d'ensembles invariants dont la dynamique transverse est conjuguée à un fer à cheval. Comment ceux-ci dégénèrent-ils vers l'ensemble minimal du piège de Kuperberg ? Le temps de retour à ces ensembles tranverses invariants devient de plus en plus long quand on s'approche du piège de Kuperberg, mais j'ignore si c'est l'unique cause de la bifurcation. Il me semble donc intéressant de comprendre ce processus.

Les résultats du deuxième chapitre ont été obtenus en collaboration avec Pierre Dehornoy. Nous avons construit une quantité associée à un champ de vecteurs X muni d'une mesure invariante μ, qui est préservée par conjugaison. Nous appelons cette quantité un invariant de (X, μ). Ce problème est motivé par une observation de Helmholtz [Hel1858] : si X_t est un champ de vecteurs non-autonome qui satisfait les équations d'Euler (dans le cas plus simple de ces équations) et si on note ϕ_t son flot, alors $\mathrm{rot}(X_t)$ est l'image sous ϕ_t de $\mathrm{rot}(X_0)$. Comme ϕ_t est un difféomorphisme

qui préserve un volume, un invariant appliqué à $\mathrm{rot}(X_0)$ nous donne une quantité qui ne dépend pas du temps pour les solutions de l'équation d'Euler.

L'invariant le plus connu est l'hélicité, il est défini quand la mesure invariante μ est un volume. Grâce aux travaux d'Arnold [Arn73], nous avons une interprétation topologique de cet invariant : dans $\mathbb{S}^3$ (ou un domaine simplement connexe de $\mathbb{R}^3$), l'hélicité coïncide avec le nombre d'enlacement asymptotique. Ce nombre est défini de la façon suivante. Prenons deux points $x_1, x_2 \in \mathbb{S}^3$ et deux nombres $t_1, t_2 \in \mathbb{R}$. On considère les courbes $k(x_i, t_i)$, pour $i = 1, 2$, formées par le segment d'orbite entre x_i et $\phi_{t_i}(x_i)$ suivi d'un arc (court) entre ces deux points. On peut montrer [Vog02] que pour presque toute paire de points et pour presque toute paire de nombres réels, on obtient deux courbes fermées simples et disjointes. Nous pouvons donc calculer leur nombre d'enlacement $\ell(k(x_1, t_1), k(x_2, t_2))$. L'hélicité est alors égale à

$$\int\int \left(\lim_{t_1, t_2 \to \infty} \frac{\ell(k(x_1, t_1), k(x_2, t_2))}{t_1 t_2} \right) d\mu d\mu.$$

Si μ est une mesure ergodique, nous n'avons pas besoin d'intégrer. Cette interprétation nous dit que l'hélicité est un invariant asymptotique : elle peut être obtenue comme la limite d'un invariant des entrelacs. Il semble donc naturel d'imiter cettte construction pour d'autres invariants de nœuds ou entrelacs, pour trouver d'autres invariants asymptotiques. Cette voie a été explorée par Gambaudo et Ghys [GG01], Baader [Baa11] et Baader et Marché [BM12], pour différents invariants des nœuds. Mais tous les invariants obtenus par ces auteurs sont proportionnels à l'hélicité.

Récemment, Kudryavtseva [Kud14, Kud16] et Enciso, Peralta-Salas et Torres de Lizaur [EPT16] ont montré sous différentes hypothèses, que tout invariant dont la dérivée de Fréchet est l'intégrale d'un noyau continu, est une fonction de l'hélicité. Donc, si l'on cherche de nouveaux invariants, ils ne peuvent pas être trop réguliers.

Nous avons décidé d'étudier un invariant des nœuds appelé le tronc, introduit par Ozawa [Ozw10]. Cet invariant est construit en comptant le nombre de points d'intersection entre un nœud et les niveaux d'une fonction *hauteur*. Dans le cas de $\mathbb{S}^3$, une fonction hauteur a deux points singuliers et tout autre niveau est une sphère. Une adaptation naturelle au cas des champs de vecteurs est le *flux géometrique* à travers les niveaux de la fonction. Il s'agit de mesurer par rapport à une mesure invariante, le passage infinitésimal à travers la surface sans considérer l'orientation.

L'invariant qui en résulte est un invariant par conjugaison topologique, et il admet une interprétation asymptotique : dans le cas d'une mesure ergodique, il s'agit de la limite du tronc de $k(x, t)$ divisé par t, pour presque tout $x \in \mathbb{S}^3$. Je présente dans le chapitre 2 les résultats que nous avons obtenus concernant cet invariant, en particulier, nous pouvons montrer qu'il n'est pas proportionnel à l'hélicité. Dans la section 2.1, j'ai décidé d'inclure le calcul qui nous permet de montrer cette dernière affirmation.

Chapter 1

A minimal set

A 3-dimensional closed manifold has Euler characteristic zero, meaning that it admits a non-singular vector field. There is one known way to build C^∞ or real analytic flows without fixed points and without periodic orbits that applies to any of these manifolds: using *Kuperberg plugs*. A plug allows to modify a flow inside a flow-box, trapping orbits and introducing at least a minimal set.

K. Kuperberg's construction appeared in 1993, published in 1994 [Kup94]. The article was then followed by a Séminaire Bourbaki exposition by É. Ghys [Ghys95], a Sugaku lecture by S. Matsumoto [Mat95] and a paper by Greg and Krystyna Kuperberg [KK96]. Each of these papers gives different insights into the dynamics of Kuperberg flows, I will explain briefly some of them in Section 1.2.2. Regarding the minimal set of the flow inside the plug, it was known that there is only one minimal set and there where examples for which its dimension is 2.

In [P5], S. Hurder and I went into the details of these flows, trying to understand what the minimal set looks like. I will give here an informal description of it and cite the main results of our work, mainly related to its shape properties and some types of entropy of the flow. To my knowledge, our work gives the first explicit example of an exceptional minimal set of a flow that has topological dimension 2 and is not obtained from a suspension of a diffeomorphism. This minimal set has amazing properties, some of them explained below. We developed a set of *ad-hoc* techniques for studying it. I ignore if any of these can be applied to other minimal sets.

The chapter is organized as follows. Sections 1.1 and 1.2 are a brief introduction to the problem and the results on Kuperberg flows previous to our work. Section 1.2 is divided into the original construction by K. Kuperberg explained in Section 1.2.1 and some known results on their dynamics other than aperiodicity explained in Section 1.2.2. In Section 1.3 and its subsections, I tried to give a picture of the minimal set. In Section 1.3.1, I start by explaining the structure of two special orbits of the flow, then in Section 1.3.2 I use these two orbits to decompose a dense subset of the minimal set whose dimension is 2. This is not a formal exposition since it avoids several minor complications and I refer for the proofs of the facts used to [P5].

In the paper [P5] we used several pseudogroups acting on a rectangle that is almost transverse to the flow of the Kuperberg plug to study the dynamics beyond aperiodicity. Even if in this text I don't present any proof using pseudogroups, I included in Section 1.4 the choice of the rectangle and some of the maps we studied in [P5]. These maps then appear in the discussions in Sections 1.4.2 and 1.5.

Section 1.5 corresponds to the results obtained in [P7]. Kuperberg flows have topological entropy zero, as a consequence of Katok's theorem on C^2-flows [Kat80]. The question that motivated the results in [P7] was whether there are positive topological entropy flows arbitrarily near the Kuperberg flows. The answer is yes in the C^1-topology by more general results on 3-dimensional

flows. Since the Kuperberg examples are explicit, it seemed that we could work in the C^∞-topology. The answer is again yes: we found an explicit construction of a 1-parameter family containing a Kuperberg flow and flows of positive topological entropy. I give the construction highlighting the difference with the original construction by K. Kuperberg and explain the main ideas in the proof.

1.1 The Seifert conjecture, a story beyond Wilson, Schweitzer and Kuperberg

In 1950, Seifert proved that vector fields close to a vector field tangent to the Hopf fibration have periodic orbits [Sei1950]. He asked whether any non-singular vector field on the three sphere $\mathbb{S}^3$ had a periodic orbit, the positive answer to this question became known as the Seifert conjecture.

When studying a vector field on a manifold, the first relevant question is to know if it has zeros. To each isolated zero of the vector field we can associate an integer index, and the Poincaré-Hopf theorem tell us, that the sum of the indeces is equal to the Euler characteristic of the manifold. After Seifert result, there was the hope to find an analog of the Poincaré-Hopf theorem for periodic orbits. The result by F. W. Wilson mentioned below killed the hope to find such an index in dimension greater than 3, and then the results by P. Schweitzer and K. Kuperberg imply that there is no analog in dimension 3.

In 1966, F. W. Wilson built a plug that allows to obtain on any closed 3-manifold a non-singular vector field with a finite number of periodic orbits [Wil66, PW77] (the construction in the second paper is simpler). Moreover, this can be donne in any homotopy class of vector fields. That is, any homotopy class of non-singular vector fields contains a vector field with a finite number of periodic orbits. For manifolds of dimension strictly greater than 3, Wilson's construction provides a vector field without periodic orbits; at the place of the finite number of periodic orbits in dimension 3, in dimension $n > 3$ the construction gives a finite number of invariant $n-2$ dimensional tori endowed with an aperiodic flow. Thus on any closed manifold of dimension $n > 3$ with Euler characteristic zero, each homotopy class of non-singular vector fields contains a vector field without periodic orbits.

Back to dimension 3, after Wilson's result the problem was how to destroy those periodic orbits and there was a possible path: to build a plug without periodic orbits.

To fix ideas, let me define a plug. A 3-dimensional plug is a manifold P endowed with a vector field $\mathcal{X}$ satisfying the following properties: the manifold P is of the form $D \times [-2, 2]$, where D is a compact 2-manifold with boundary ∂D. Let $\frac{\partial}{\partial z}$ be the *vertical* vector field on P, where z is the coordinate on $[-2, 2]$. The vector field $\mathcal{X}$ on P must satisfy the conditions:

- (P1) *vertical near the boundary*: $\mathcal{X} = \frac{\partial}{\partial z}$ in a neighborhood of ∂P; thus, $D \times \{-2\}$ and $D \times \{2\}$ are the entry and exit regions of P for the flow of $\mathcal{X}$, respectively;
- (P2) *entry-exit condition*: if a point $(x, -2)$ is in the same trajectory as $(y, 2)$, then $x = y$. That is, an orbit that traverses P, exits just in front of its entry point;
- (P3) *trapped orbit*: there is at least one entry point whose entire *forward* orbit is contained in P; we will say that its orbit is *trapped* by P and we call the set of entry points with trapped orbit the *trapped set*;
- (P4) *tameness*: there is an embedding $i\colon P \to \mathbb{R}^3$ that preserves the vertical direction on the boundary ∂P.

A plug is *aperiodic* if there is no closed orbit for $\mathcal{X}$. After Wilson's result an aperiodic plug will allow to build a vector field without periodic orbits. Indeed, we can use such a plug to destroy the periodic orbits one by one. Consider one periodic orbit, it suffices to embed the aperiodic plug in a flow-box intersecting the periodic orbit in such a way that the periodic orbit gets trapped inside the plug, thus it will no longer be periodic. This can be done by conditions (P1), (P3) and

(P4). Condition (P2) guarantees that there are no new periodic orbits after surgery: there are no periodic orbits inside the plug and if an orbit intersects the plug and is not trapped, the entry-exit condition implies that it will stay periodic or non-periodic after surgery. Repeating this process at most finitely many times, gives an aperiodic flow on any closed 3-manifold.

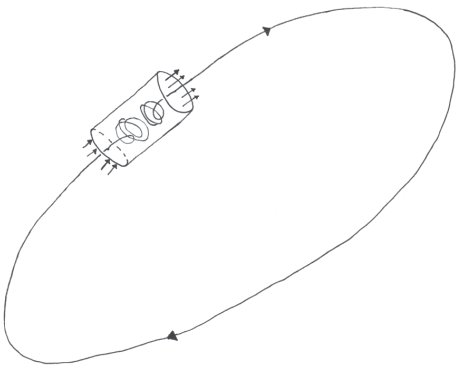

Figure 1.1: A plug trapping a periodic orbit

The first aperiodic plug was built by P. Schweitzer [Sch74] in 1974, though the flow is only C^1. The aperiodic plug that is C^∞ (and even real analytic) was built by K. Kuperberg in 1993 [Kup94]. In both cases, the use of the plugs gives a vector field that is homotopic (through non-singular vector fields) to the original one. Hence, the surgery does not changes the homotopy class of the vector field. Notice that almost 20 years passed between the two constructions, in the meantime J. Harrison managed to make a C^2 version of Schweitzer's plug [Har88] and there are a couple of papers trying to prove that it is impossible to build an aperiodic plug with a smooth flow. But how to prove that there are no aperiodic plugs in the C^r category for $r > 2$?

Let me highlight one of the main differences between Schweitzer's and Kuperberg's construction. Condition (P3) in the definition of a plug implies that a trapped orbit has to accumulate on an invariant set, thus a plug contains a minimal set for the flow. Schweitzer's construction starts with a minimal set: the main idea is to substitute the periodic orbits in the Wilson plug with two copies of the Denjoy minimal set. The differentiability problem comes from this set. J. Harrison changed the embedding of the minimal set to make the flow C^2. Kuperberg's construction focuses on destroying the periodic orbits of the Wilson plug, there is some minimal set in the plug, but not too much was known about it before our work. I will cite S. Matsumoto [Mat95] to describe K. Kuperberg's construction:

> We therefore must demolish the two closed orbits in the Wilson Plug beforehand. But producing a new plug will take us back to the starting line. The idea of Kuperberg is to let closed orbits demolish themselves. We set up a trap within enemy lines and watch them settle their dispute while we take no active part.

After Schweitzer's construction the idea to prove that it was impossible to build a C^∞ aperiodic plug concentrates on the minimal set inside the plug (the starting point of his construction). I want to mention a paper by M. Handel [Han80], in which he proves that if the trapped orbits of a plug accumulate on a minimal set whose dimension is 1 and this is the only invariant set for the flow in the plug, then the minimal set is *surface-like*: the flow restricted to the minimal set is topologically conjugated to the minimal set of a flow on a surface. He considers also the case of a minimal set whose topological dimension is two, but he makes the assumption that there is a disk-like section of the minimal set. In Kuperberg's plug the minimal set is not the only invariant set of the plug, as proved by S. Matsumoto (see Theorem 1.2.3), and when it has topological dimension 2 it does not admits a disk-like section.

There is also a paper by R. J. Knill that embeds Denjoy minimal sets in C^∞-flows on $\mathbb{S}^3$, but these are not isolated as any neighborhood contains periodic orbits [Kni81]. Hence, until

K. Kuperberg's construction, the idea was to look at the possible minimal sets for an aperiodic plug.

It seems a good moment to comment on two (difficult) questions. The first one is on the dimension of the minimal set of the Kuperberg plug. We proved in [P5] that, under some extra assumptions on the construction, this set has topological dimension two. We do not know if there are smooth Kuperberg flows whose minimal set has dimension 1. I have tried to build them without success. Can one prove that a minimal set with dimension 1 and unstable shape cannot be isolated (meaning that any neighborhood should contain periodic orbits)? The answer to this question is yes if the minimal set is a solenoid as proved by E. S. Thomas [Tho73].

Secondly, consider the case of volume preserving flows on 3-manifolds. We are at the stage of knowing that there are examples with a finite number of periodic orbits and C^1 examples without periodic orbits on any closed 3-manifold. These were built by G. Kuperberg [Kup96]. Is it possible to build a C^∞ volume preserving aperiodic plug? Can we a priori say something about its minimal or invariant sets?

1.2 Kuperberg's construction and previous results

As mentioned above, K. Kuperberg's idea is to destroy the periodic orbits in the modified Wilson's plug using the plug itself, or let the periodic orbits demolish themselves. So I start explaining how to build Wilson plug (actually a modified version of the original plug). The construction of the self-insertions that destroy the periodic orbits is explained in Section 1.2.1.

Consider the rectangle

$$\mathbf{R} = [1,3] \times [-2,2] = \{(r,z) \mid 1 \le r \le 3 \ \& \ -2 \le z \le 2\}.$$

Choose a C^∞-function $g\colon \mathbf{R} \to [0, g_0]$ for $g_0 > 0$, which satisfies the "vertical" symmetry condition $g(r,z) = g(r,-z)$. Also, require that $g(2,-1) = g(2,1) = 0$ and that $g(r,z) > 0$ otherwise. Define the vector field $\mathcal{W}_v = g \cdot \frac{\partial}{\partial z}$ which has two singularities, $(2, \pm 1)$ and is otherwise everywhere vertical, as illustrated in Figure 1.2.

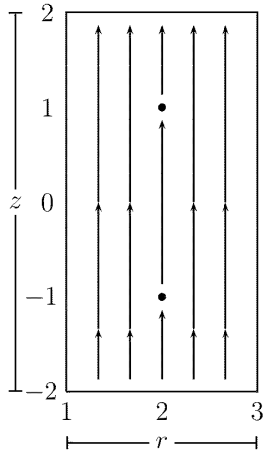

Figure 1.2: Vector field $\mathcal{W}_v$

Next, choose a C^∞-function $f\colon \mathbf{R} \to [-1,1]$ which satisfies the following conditions:

(W1) $f(r,-z) = -f(r,z)$ [*anti-symmetry in z*].
(W2) $f(\xi) = 0$ for ξ near the boundary of $\mathbf{R}$.
(W3) $f(r,z) \ge 0$ for $-2 \le z \le 0$.
(W4) $f(r,z) \le 0$ for $0 \le z \le 2$.
(W5) $f(2,-1) = 1$ and $f(2,1) = -1$.

Next, define the manifold with boundary

$$\mathbb{W} = [1,3] \times \mathbb{S}^1 \times [-2,2] \cong \mathbf{R} \times \mathbb{S}^1 \qquad (1.1)$$

with cylindrical coordinates $x = (r, \theta, z)$. That is, $\mathbb{W}$ is a solid cylinder with an open core removed, obtained by rotating the rectangle $\mathbf{R}$, considered as embedded in $\mathbb{R}^3$, around the z-axis.

Extend the functions f and g above to $\mathbb{W}$ by setting $f(r,\theta,z) = f(r,z)$ and $g(r,\theta,z) = g(r,z)$, so that they are invariant under rotations around the z-axis. The *modified Wilson vector field* $\mathcal{W}$ on $\mathbb{W}$ is defined by

$$\mathcal{W} = g(r,\theta,z)\frac{\partial}{\partial z} + f(r,\theta,z)\frac{\partial}{\partial \theta} \ . \qquad (1.2)$$

Let Ψ_t denote the flow of $\mathcal{W}$ on $\mathbb{W}$. Observe that the vector field $\mathcal{W}$ is vertical near the boundary of $\mathbb{W}$ and is horizontal at the points $(r, \theta, z) = (2, \theta, \pm 1)$. Also, $\mathcal{W}$ is tangent to the cylinders $\{r = cst.\}$. The flow Ψ_t on the cylinders $\{r = cst.\}$ is illustrated by Figure 1.3.

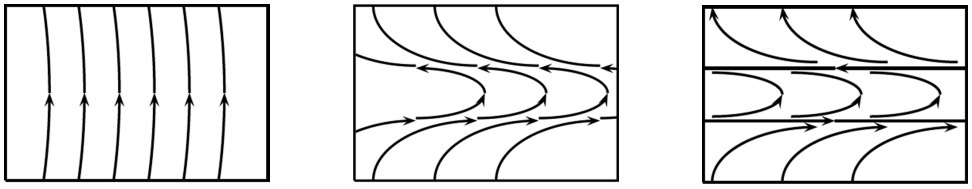

Figure 1.3: $\mathcal{W}$-orbits on the cylinders $\{r = cst.\}$

Define the closed subsets:

$$\begin{aligned}
\mathcal{R} &= \{(2, \theta, z) \mid -1 \leq z \leq 1\} \quad [\textit{The Reeb Cylinder}] \\
\mathcal{A} &= \{z = 0\} \quad [\textit{The Center Annulus}] \\
\mathcal{O}_i &= \{(2, \theta, (-1)^i)\} \quad [\textit{Periodic Orbits, i=1,2}] \\
\partial_h^- \mathbb{W} &= \{(r, \theta, -2)\} \quad [\textit{The Entry Region}] \\
\partial_h^+ \mathbb{W} &= \{(r, \theta, 2)\} \quad [\textit{The Exit Region}]
\end{aligned}$$

Then $\mathcal{O}_1$ is the lower boundary circle of the Reeb cylinder $\mathcal{R}$ and $\mathcal{O}_2$ is the upper boundary circle. The flow Ψ_t has exactly two periodic orbits $\mathcal{O}_1$ and $\mathcal{O}_2$, the maximal invariant set inside the plug is the Reeb cylinder $\mathcal{R}$ and satisfies the entry-exit condition (P2) as a consequence of the symmetry in the function g and condition (W1). Finally, observe that the trapped set are the points with $r = 2$ in the entry region of $\mathbb{W}$.

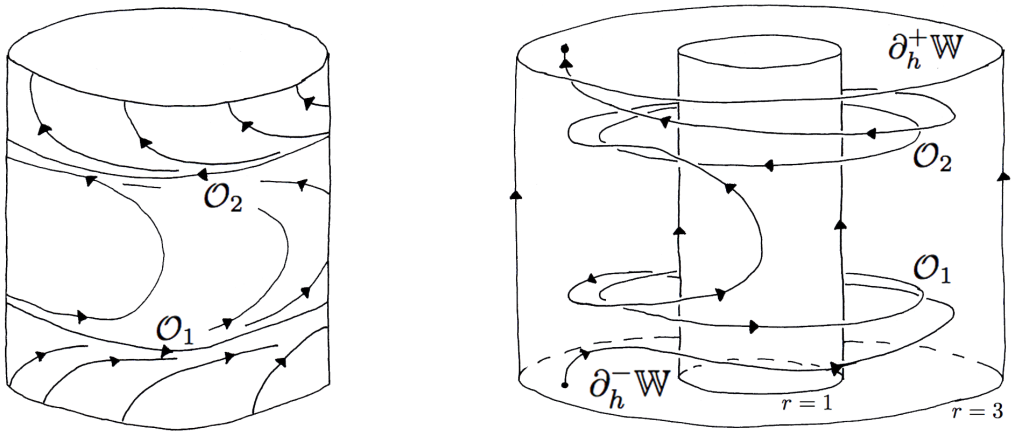

Figure 1.4: $\mathcal{W}$-orbits on the cylinder $\{r = 2\}$ and in $\mathbb{W}$

1.2.1 The Kuperberg plug $\mathbb{K}$

The construction of the Kuperberg Plug begins with the modified Wilson Plug $\mathbb{W}$ with vector field $\mathcal{W}$. The first step is to re-embed the manifold $\mathbb{W}$ in $\mathbb{R}^3$ as a *folded figure-eight*, as shown in Figure 1.5, preserving the vertical direction.

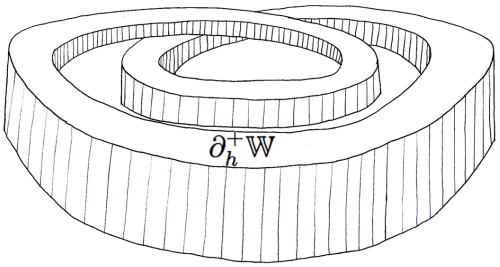

Figure 1.5: Embedding of Wilson Plug $\mathbb{W}$ as a *folded figure-eight*

The fundamental idea of the Kuperberg Plug is to construct two insertions of $\mathbb{W}$ into itself, in such a way that the two periodic orbits will be trapped by these self-insertions. Moreover, the insertions are made so that the resulting space $\mathbb{K}$ is again embedded in $\mathbb{R}^3$. A key subtlety of the construction arises in the precise requirements on these self-insertions. As with the construction of the modified Wilson Plug, the description of this construction in the works [Kup94, Ghys95, Mat95] is qualitative, as this suffices to prove the aperiodicity of the resulting flow. As explained in [P5], other properties of the dynamics of the flow Φ_t in the resulting plug $\mathbb{K}$ are strongly influenced by the precise nature of these maps, so some hypotheses were added to the construction. We call a plug satisfying these hypotheses a generic Kuperberg plug and its flow a generic Kuperberg flow. In Remark 1.2.1 at the end of this section I briefly explain the generic hypotheses and in Section 1.6 I give a compilation of the generic hypotheses.

After the embedding presented in Figure 1.5, the construction continues with the choice in the annulus $[1,3]\times\mathbb{S}^1$ of two closed regions L_i, for $i=1,2$, which are topological disks. Each region has boundary defined by two arcs: for $i=1,2$, α_i' is the boundary contained in the interior of $[1,3]\times\mathbb{S}^1$ and α_i in the outer boundary contained in the circle $\{r=3\}$, as depicted in Figure 1.6.

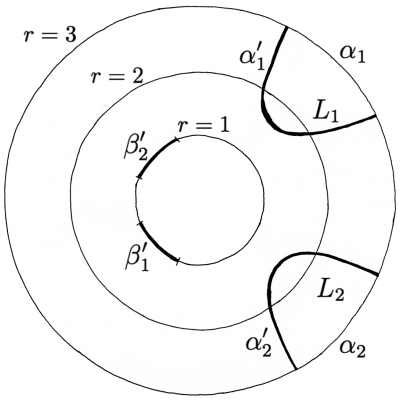

Figure 1.6: The disks L_1 and L_2

Consider the closed sets $D_i = L_i\times[-2,2]\subset\mathbb{W}$, for $i=1,2$. Note that each D_i is homeomorphic to a closed 3-ball, that $D_1\cap D_2=\emptyset$ and each D_i intersects the cylinder $\{r=2\}$ in a rectangle. Label the top and bottom faces of these regions by

$$L_1^{\pm} = L_1\times\{\pm 2\}\ ,\ L_2^{\pm} = L_2\times\{\pm 2\}\ . \quad (1.3)$$

The next step is to define insertion maps $\sigma_i\colon D_i\to\mathbb{W}$, for $i=1,2$, in such a way that the periodic orbits $\mathcal{O}_i$ flow Ψ_t intersect $\sigma_i(L_i^-)$ in points corresponding to $\mathcal{W}$-trapped entry points for the Wilson plug $\mathbb{W}$. Consider two disjoint arcs β_i' in the inner boundary circle $\{r=1\}$, that are in front of the arcs α_i when the plug is embedded as in Figure 1.5. For $i=1,2$, choose orientation preserving diffeomorphisms $\sigma_i\colon\alpha_i'\to\beta_i'$ and extend these maps to smooth embeddings $\sigma_i\colon D_i\to\mathbb{W}$, as illustrated in Figure 1.7, which satisfy the conditions:

(K1) $\sigma_i(\alpha_i'\times z)=\beta_i'\times z$ for $z\in[-2,2]$, the interior arc α_i' is mapped to a boundary arc β_i';
(K2) for $\mathcal{D}_i=\sigma_i(D_i)$, $\mathcal{D}_1\cap\mathcal{D}_2=\emptyset$;
(K3) $\sigma_1(L_1^-)\subset\{z<0\}$ and $\sigma_2(L_2^+)\subset\{z>0\}$;
(K4) For every $x\in L_i$, the image $\sigma_i(x\times[-2,2])$ is an arc contained in a trajectory of $\mathcal{W}$;
(K5) Each slice $\sigma_i(L_i\times\{z\})$ is transverse to the vector field $\mathcal{W}$, for all $-2\le z\le 2$;

(K6) $\mathcal{D}_i$ intersects the periodic orbit $\mathcal{O}_i$ and not $\mathcal{O}_j$, for $i \neq j$.

For $i = 1, 2$, the components of the boundary of the embedded regions $\mathcal{D}_i = \sigma_i(D_i) \subset \mathbb{W}$ that are transverse to $\mathcal{W}$ are labeled by

$$\mathcal{L}_i^{\pm} = \sigma_i(L_i^{\pm}) \ . \tag{1.4}$$

Note that the arcs $\sigma_i(x \times [-2, 2])$ in condition (K3) are line segments from $\sigma_i(x \times \{-2\}) \in \mathcal{L}_i^-$ to $\sigma_i(x \times \{2\}) \in \mathcal{L}_i^+$ which follow the $\mathcal{W}$-trajectory and traverse the insertion from the bottom face to the top face. Since $\mathcal{W}$ is vertical near the boundary of $\mathbb{W}$ and horizontal at the two periodic orbits, we have that the arcs $\sigma_i(x \times [-2, 2])$ are vertical near the inserted curve $\sigma_i(\alpha_i')$ and horizontal at the intersection of the insertion with the periodic orbit $\mathcal{O}_i$. Thus, the embeddings of the surfaces $\sigma_i(L_i \times \{z\})$ make a *half turn* upon insertion, for each $-2 \leq z \leq 2$. The turning is clockwise for the bottom insertion $i = 1$ as illustrated in Figure 1.7 and counter-clockwise for the upper insertion $i = 2$, which is illustrated in Figure 1.9.

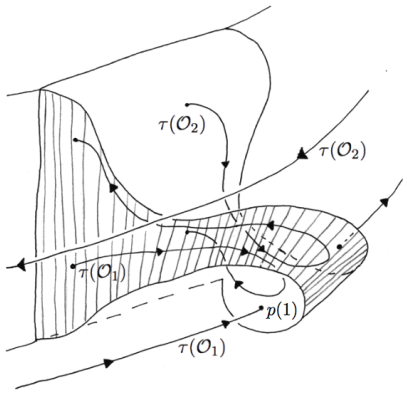

Figure 1.7: The image of D_1 under σ_1

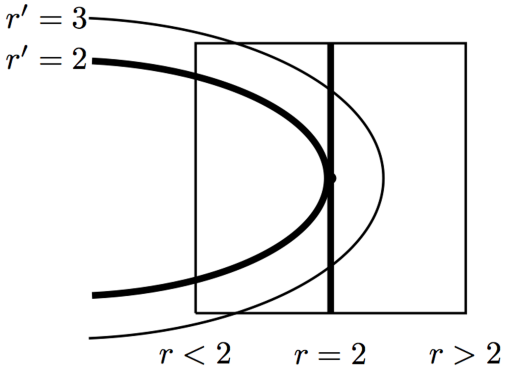

Figure 1.8: The radius inequality

The embeddings σ_i are also required to satisfy two further conditions, which are the key to showing that the resulting Kuperberg flow Φ_t is *aperiodic*:

(K7) For $i = 1, 2$, the disk L_i contains a point $(2, \theta_i)$ such that the image under σ_i of the vertical segment $(2, \theta_i) \times [-2, 2] \subset D_i \subset \mathbb{W}$ is an arc of the periodic orbit $\mathcal{O}_i$ of $\mathcal{W}$.

(K8) *Radius Inequality*: For all $x = (r', \theta', z') \in L_i \times [-2, 2]$, let $(r, \theta, z) = \sigma_i(r', \theta', z') \in \mathcal{D}_i$, then $r' > r$ unless $x = (2, \theta_i, z)$.

The Radius Inequality (K8), illustrated in Figure 1.8, is one of the most fundamental concepts of Kuperberg's construction. This is an "idealized" case, as it implicitly assumes that the relation between the values of r and r' is "quadratic" in a neighborhood of the special points $(2, \theta_i)$, which is not required in order that (K8) be satisfied. This "quadratic condition" is part of the generic hypotheses on the construction (see Remark 1.2.1 and Hypothesis 1.6.3).

The Radius Inequality (K8) is a monotone condition that allows to keep track of the behavior of the orbits in the Kuperberg plug. It is this condition that is violated in the construction in Section 1.5.

The embeddings $\sigma_i \colon L_i \times [-2, 2] \to \mathbb{W}$, for $i = 1, 2$, can be constructed by first choosing smooth embeddings of the faces $\sigma_i \colon L_i^- \to \mathbb{W}$ so that the image surfaces are transverse to the vector field $\mathcal{W}$ on $\mathbb{W}$ and satisfy the conditions (K1), (K5) for $z = -2$, (K7) and (K8). Then we extend the embeddings of the faces L_i^- to the sets $L_i \times [-2, 2]$ by flowing the images using a reparametrization of the flow of $\mathcal{W}$, so that we obtain embeddings of $L_i \times [-2, 2]$ satisfying conditions (K1) to (K8), as pictured in Figure 1.7 for the bottom insertion.

Finally, define $\mathbb{K}$ to be the quotient manifold obtained from $\mathbb{W}$ by identifying the sets D_i with $\mathcal{D}_i$. That is, for each point $x \in D_i$ identify x with $\sigma_i(x) \in \mathbb{W}$, for $i = 1, 2$, as illustrated in Figure 1.9. The restricted Ψ_t-flow on the inserted disk $\mathcal{D}_i = \sigma_i(D_i)$ is not compatible with the image of the restricted Ψ_t-flow on D_i. Thus it is necessary to modify $\mathcal{W}$ on each insertion $\mathcal{D}_i$, by replacing the vector field $\mathcal{W}$ on the interior of each region $\mathcal{D}_i$ with the image vector field, so that the dynamics in the interior of each insertion region $\mathcal{D}_i$ reverts back to the Wilson dynamics on D_i. As for the insertion of plugs, the flow has to be reparametrized near the boundary of the insertion so that the resulting flow is C^∞. Let $\mathcal{K}$ be the resulting vector field and Φ_t its flow.

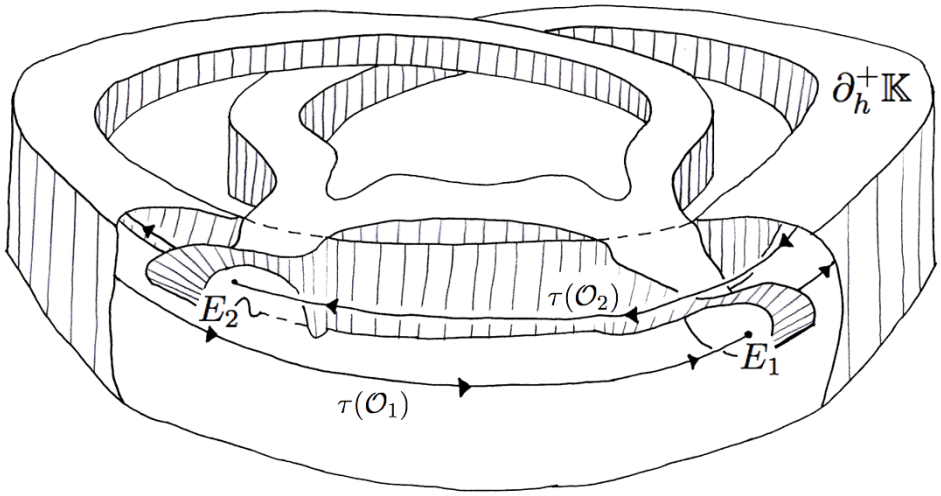

Figure 1.9: The Kuperberg Plug $\mathbb{K}$

REMARK 1.2.1 (The generic hypotheses)**.** *Under the name generic hypotheses, we added in [P5] a set of conditions to the constructions of the modified Wilson plug $\mathbb{W}$ and the Kuperberg plug $\mathbb{K}$ that allowed us to study the dynamics of the flows beyond aperiodicity. Some of these are technical assumptions and can be classified into two classes:*

- *The function g in the construction of the modified Wilson plug $\mathbb{W}$ is zero only at the points $(2, \pm 1)$ of the rectangle and the speed at which it goes to zero near this points is specified in the generic hypotheses: we ask g to be a quadratic function of the distance to these points (in a small neighborhood).*
- *The Radius Inequality (K8) is required to be quadratic near the special points, as suggested by Figure 1.8.*

These assumptions are used to prove that the minimal set in the plug has topological dimension 2 (see Chapter 17 of [P5]), to give explicit computations of the topological entropy of the flow restricted to the minimal set (see Chapters 20 and 21 of [P5]) and to justify the description of the minimal set (see Chapter 18 of [P5]).

Recently, D. Ingebretson used the generic hypotheses to interpret the minimal set as the minimal set of an iterated function system and compute its Hausdorff dimension [HI].

1.2.2 Notation and basic results on the dynamics

In this section, I introduce notations that will be used throughout this chapter. The notation used here is the same as in [P5]. Introduce the sets:

$$\mathbb{W}' \;=\; \mathbb{W} - \{\mathcal{D}_1 \cup \mathcal{D}_2\} \quad , \quad \widehat{\mathbb{W}} \;=\; \overline{\mathbb{W} - \{\mathcal{D}_1 \cup \mathcal{D}_2\}}\ . \tag{1.5}$$

The compact space $\widehat{\mathbb{W}} \subset \mathbb{W}$ is the result of "drilling out" the interiors of $\mathcal{D}_1$ and $\mathcal{D}_2$.

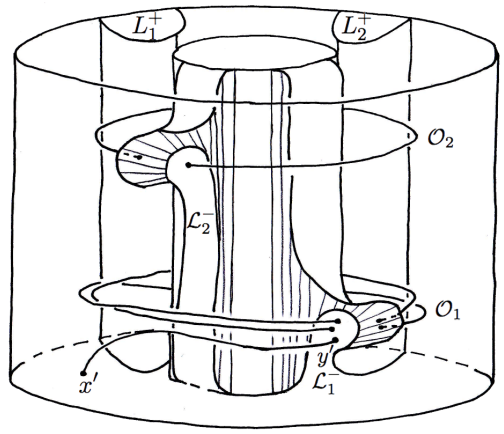

Figure 1.10: $\widehat{\mathbb{W}}$ with some Wilson arcs

For $x, y \in \mathbb{K}$, we say that $x \prec_{\mathcal{K}} y$ if there exists $t \geq 0$ such that $\Phi_t(x) = y$. Likewise, for $x', y' \in \mathbb{W}$, we say that $x' \prec_{\mathcal{W}} y'$ if there exists $t \geq 0$ such that $\Psi_t(x') = y'$.

Let $\tau\colon \mathbb{W} \to \mathbb{K}$ denote the quotient map, which for $i = 1, 2$, identifies a point $x \in D_i$ with its image $\sigma_i(x) \in \mathcal{D}_i$. Then the restriction $\tau'\colon \mathbb{W}' \to \mathbb{K}$ is injective and onto. Let $(\tau')^{-1}\colon \mathbb{K} \to \mathbb{W}'$ denote the inverse map, which followed by the inclusion $\mathbb{W}' \subset \mathbb{W}$, yields the (discontinuous) map $\tau^{-1}\colon \mathbb{K} \to \mathbb{W}$. For $x \in \mathbb{K}$, let $x = (r, \theta, z)$ be defined as the $\mathbb{W}$-coordinates of $\tau^{-1}(x) \subset \mathbb{W}'$. In this way, we obtain (discontinuous) coordinates (r, θ, z) on $\mathbb{K}$. In particular, let $r\colon \mathbb{W}' \to [1, 3]$ be the restriction of the radius coordinate on $\mathbb{W}$, then the function is extended to the *radius function* of $\mathbb{K}$, again denoted by r, where for $x \in \mathbb{K}$ set $r(x) = r(\tau^{-1}(x))$.

The flow of the vector field $\mathcal{W}$ on $\mathbb{W}$ preserves the radius function on $\mathbb{W}$, so $x' \prec_{\mathcal{W}} y'$ implies that $r(x') = r(y')$. However, $x \prec_{\mathcal{K}} y$ need not imply that $r(x) = r(y)$. The points of discontinuity for the function $t \mapsto r(\Phi_t(x))$ play a fundamental role in the study of the dynamics of Kuperberg flows.

Figure 1.10, copied from Ghys' paper [Ghys95], is fundamental for the understanding of the Kuperberg plug $\mathbb{K}$. Indeed, an orbit in $\mathbb{K}$ can be chopped into segments of $\mathcal{W}$-orbits, or in other words into segments of orbits in $\widehat{\mathbb{W}}$ whose endpoints lie in the boundary $\partial\widehat{\mathbb{W}}$. Thus, up to identification of $L_i^{\pm}$ with $\mathcal{L}_i^{\pm}$, Figure 1.10 contains all the information needed to follow the $\mathcal{K}$-orbits. This is the technique used to study the dynamics inside $\mathbb{K}$, as explained below or in any of the references [Ghys95, KK96, Kup94, Mat95, P5].

Let $\partial_h^-\mathbb{K} = \tau(\partial_h^-\mathbb{W} \setminus (L_1^- \cup L_2^-))$ and $\partial_h^+\mathbb{K} = \tau(\partial_h^+\mathbb{W} \setminus (L_1^+ \cup L_2^+))$ denote the bottom and top horizontal faces of $\mathbb{K}$, respectively. That is, the entry and exit regions of $\mathbb{K}$. Points $x' \in \partial_h^-\mathbb{W}$ and $y' \in \partial_h^+\mathbb{W}$ are said to be *facing*, we write $x' \equiv y'$, if $x' = (r, \theta, -2)$ and $y' = (r, \theta, 2)$ for some r and θ. The entry/exit property of the Wilson flow is then equivalent to the property that $x' \equiv y'$ if $[x', y']_{\mathcal{W}}$ is an orbit from $\partial_h^-\mathbb{W}$ to $\partial_h^+\mathbb{W}$ whenever $r(x') \neq 2$. There is also a notion of facing points for $x, y \in \mathbb{K}$, if either of two cases are satisfied:

— For $x = \tau(x') \in \partial_h^-\mathbb{K}$ and $y = \tau(y') \in \partial_h^+\mathbb{K}$, if $x' \equiv y'$ then $x \equiv y$.

— For $i = 1, 2$, with $x = \sigma_i(x')$ and $y = \sigma_i(y')$, if $x' \equiv y'$ then $x \equiv y$.

Consider the embedded disks $\mathcal{L}_i^{\pm} \subset \mathbb{W}$ defined by (1.4), which appear as the faces of the insertions in $\widehat{\mathbb{W}}$ in Figure 1.10 that are transverse to the vector field $\mathbb{W}$. Their images in the quotient manifold $\mathbb{K}$ are denoted by:

$$E_1 = \tau(\mathcal{L}_1^-)\ ,\ S_1 = \tau(\mathcal{L}_1^+)\ ,\ E_2 = \tau(\mathcal{L}_2^-)\ ,\ S_2 = \tau(\mathcal{L}_2^+)\ . \tag{1.6}$$

Note that $\tau^{-1}(E_i) = L_i^-$, while $\tau^{-1}(S_i) = L_i^+$. The *transition points* of an orbit of $\mathcal{K}$ are those

points where the orbit intersects E_1, E_2, S_1, S_2 or a boundary component $\partial_h^-\mathbb{K}$ or $\partial_h^+\mathbb{K}$. They are then either *primary* or *secondary* transition points, where $x \in \mathbb{K}$ is:

— a *primary entry point* if $x \in \partial_h^-\mathbb{K}$ or a *primary exit point* if $x \in \partial_h^+\mathbb{K}$;

— a *secondary entry point* if $x \in E_1 \cup E_2$ or a *secondary exit point* if $x \in S_1 \cup S_2$.

If a $\mathcal{K}$-orbit contains no transition points, then it lifts under τ^{-1} to a $\mathcal{W}$-orbit in $\mathbb{W}$ flowing from $\partial_h^-\mathbb{W}$ to $\partial_h^+\mathbb{W}$.

The *special points* for the flow Φ_t are the images, for $i = 1, 2$,

$$p(i) = \tau(\mathcal{O}_i \cap \mathcal{L}_i^-) \in E_i \ , \ \overline{p}(i) = \tau(\mathcal{O}_i \cap \mathcal{L}_i^+) \in S_i \ . \tag{1.7}$$

Then $p(i) \equiv \overline{p}(i)$ for $i = 1, 2$ and by the Radius Inequality (K8), we have $r(p(i)) = r(\overline{p}(i)) = 2$ for $i = 1, 2$. The two $\mathcal{K}$-orbits containing these points are the special orbits $\mathcal{S}_i$ for $i = 1, 2$.

A $\mathcal{W}$-*arc* is a closed segment $[x, y]_{\mathcal{K}} \subset \mathbb{K}$ of the flow of $\mathcal{K}$ whose only transition points are the endpoints $\{x, y\}$. The open interval $(x, y)_{\mathcal{K}}$ is then the image under τ of a unique $\mathcal{W}$-orbit segment in $\mathbb{W}'$, denoted by $(x', y')_{\mathcal{W}}$ where $\tau(x') = x$ and $\tau(y') = y$ Let $[x', y']_{\mathcal{W}}$ denote the closure of $(x', y')_{\mathcal{W}}$ in $\widehat{\mathbb{W}}$, then we say that $[x', y']_{\mathcal{W}}$ is the *lift* of $[x, y]_{\mathcal{K}}$ and is an arc of $\mathcal{W}$-orbit as in Figure 1.10. Note that the radius function r is constant along $[x', y']_{\mathcal{W}}$.

The *level function* along a $\mathcal{K}$-orbit indexes the discontinuities of the radius function. Given $x \in \mathbb{K}$, set $n_x(0) = 0$ and for $t > 0$ define

$$n_x(t) = \#\left\{(E_1 \cup E_2) \cap \Phi_s(x) \mid 0 < s \leq t\right\} - \#\left\{(S_1 \cup S_2) \cap \Phi_s(x) \mid 0 < s \leq t\right\}. \tag{1.8}$$

That is, $n_x(t)$ is the total number of secondary entry points, minus the total number of secondary exit points, traversed by the flow of x over the interval $0 < s \leq t$. Thereafter, $n_x(t)$ changes value by ± 1 at each $t > 0$ such that $\Phi_t(x)$ is a transition point and whether the value increases or decreases, indicates whether the transition point is an entry or exit point.

The level function is the main tool for studying the dynamics of Φ_t. Consider an orbit in $\mathbb{K}$ and assume that it is not a Wilson orbit, meaning that it contains a certain number of transition points. Cutting the orbit at these points gives a sequence of $\mathcal{W}$-arcs that lift to pieces of orbit in $\widehat{\mathbb{W}}$ (as in Figure 1.10). We understand completely all the possible pieces in $\widehat{\mathbb{W}}$, thus what is important is to understand how these pieces concatenate to form an orbit in $\mathbb{K}$.

The level function measures how "deep" the orbit goes: how many entries has passed, without crossing the corresponding exit points. This allows to follow the orbit and understand the behavior of the radius coordinate. In Section 1.3.2 the level function is used in a fundamental way to understand the structure of the minimal set.

Clearly the main result on $\mathbb{K}$ is:

THEOREM 1.2.2. *$\mathbb{K}$ endowed with the vector field $\mathcal{K}$ is an aperiodic plug.*

The proof uses strongly the level function. The Radius Inequality (K8) is only used for proving that there are no periodic orbits inside the plug. We refer to any of the papers [Ghys95, KK96, Kup94, Mat95, P5] for a proof.

I also like to state a result by S. Matsumoto on the dynamics of the plug (see Proposition 7.5 of [P5] for a proof).

THEOREM 1.2.3. *The trapped set of $\mathbb{K}$ contains a set with non-empty interior.*

In particular, Theorem 1.2.3 implies that there is a "big" invariant set. In the next section I describe the minimal set, first as the closure of the special orbits, then as the closure of a 2-dimensional set $\mathfrak{M}_0$ obtained by flowing the Reeb cylinder $\tau(\mathcal{R})$ in $\mathbb{K}$. The proof of Theorem 1.2.3 implies that there is an invariant set that is larger than $\overline{\mathfrak{M}_0}$. In Chapter 16 of $\mathbb{K}$ we describe the orbits of this invariant set.

1.3 The minimal set under the generic hypotheses

The aim of this section is to give a description of the minimal set under the generic hypotheses (see Remark 1.2.1 and Section 1.6). I start by explaining how the special orbits, that is the orbits obtained after the Kuperberg surgery from the periodic orbits of the Wilson plug, behave. As remarked previously, an orbit in the Kuperberg plug $\mathbb{K}$ is a concatenation of segments of Wilson orbits whose endpoints are in the boundary of $\widehat{\mathbb{W}}$ (see Figure 1.10). These segments of $\mathcal{W}$-orbits are quite simple, thus to understand orbits in $\mathbb{K}$ one has to understand the rules of concatenation. The two special orbits have similar structure, I just treat the case of one of them. Once the structure of these is orbits is settled, the structure of the minimal set comes naturally.

The objective is to give a visual explanation of the objects mentioned above. By doing so, I will skip some complications. Some of the minor ones are the appearance of "bubbles" in the minimal set (see Chapters 15 and 18 of [P5]), the fact that the construction of $\mathbb{K}$ is not completely symmetric (see Chapter 9 of [P5] for a proof that the non-symmetry has minor effects on the dynamics). The more important one, is not proving that the generic hypotheses imply that the minimal set has topological dimension 2, as proved in Chapter 17 of [P5].

1.3.1 The special orbits

The minimal set of the plug $\mathbb{K}$ is obtained as the closure of any of the special orbits $\mathcal{S}_1$ or $\mathcal{S}_2$, these are the orbits in $\mathbb{K}$ that contain the arcs $\mathcal{O}'_i = \mathcal{O}_i \cap \mathbb{W}'$ of the periodic orbits of the Wilson plug $\mathbb{W}$. That is

$$\mathcal{S}_i = \mathcal{K}(\mathcal{O}'_i) = \{\Phi_t(x) \,|\, x \in \mathcal{O}'_i,\, t \in \mathbb{R}\},$$

observe that the endpoints of $\mathcal{O}'_i$ are the special points $p(i)$ and $\overline{p}(i)$ defined in (1.7), for $i = 1$ and 2. What follows explains why the periodic orbits of Wilson are not longer periodic after the surgery, but it is not a proof of the aperiodicity of the plug. The explanation implies also that $\mathcal{S}_2 \subset \overline{\mathcal{S}_1}$ and when carried out for $\mathcal{S}_2$ (I do not give the details) we get that $\overline{\mathcal{S}_1} = \overline{\mathcal{S}_2}$ is a minimal set. Proving that this set is the only minimal set in the plug is a harder task: it involves understanding the asymptotic behavior of every orbit that is entirely contained in $\mathbb{K}$. In Proposition 7.1 of [P5], it is proved that the ω-limit of every point in $\mathbb{K}$ whose orbit stays in $\mathbb{K}$ contains $\mathcal{S}_1$, while its α-limit contains $\mathcal{S}_2$. Thus $\Sigma = \overline{\mathcal{S}_1} = \overline{\mathcal{S}_2}$ is the unique minimal set.

We recall first from Figure 1.3 of the Wilson plug that the cylinder $\{r = 2\}$ contains the two

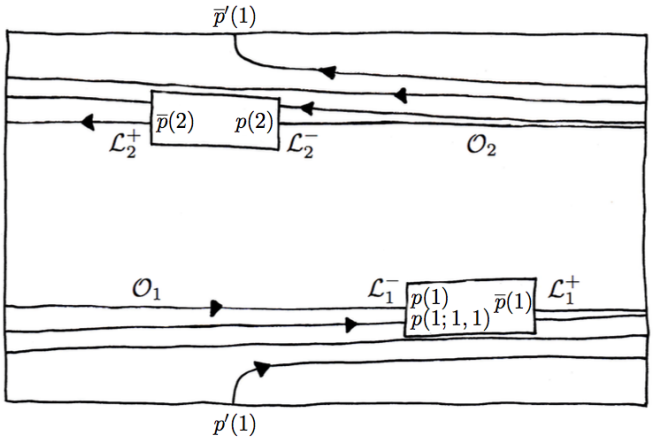

Figure 1.11: The cylinder $\{r = 2\}$ in $\widehat{\mathbb{W}}$

periodic orbits $\mathcal{O}_i$ for $i = 1, 2$. Consider the cylinder $\{r = 2\}$ in $\widehat{\mathbb{W}}$ containing the segments of orbit $\mathcal{O}'_i$ for $i = 1, 2$. Since this cylinder intersects both insertions, in Figure 1.11 I erased two regions of the rectangle, one intersecting $\mathcal{O}_1$ and the other $\mathcal{O}_2$, corresponding to each insertion. Observe that these two regions are basically rectangles, with two of their sides tangent to the vector field and two transverse to the vector field. The transverse sides are either in the entrance of the insertions $\mathcal{L}_i^-$ or in the exit of the insertions $\mathcal{L}_i^+$, for $i = 1, 2$.

The orbit segment $\overline{\mathcal{O}'_1}$ intersects the bottom entrance $\mathcal{L}_1^-$ and the bottom exit $\mathcal{L}_1^+$. Condition (K7) implies that the intersection with $\mathcal{L}_1^-$ is at the special point $p(1)$ that is identified with the point $p'(1) = (2, \theta_1, -2) \in L_1^- \cap \{r = 2\}$. That is $\sigma_1(p'(1)) = p(1)$, $\tau(p(1)) = \tau(p'(1))$ and $r(p'(1)) = 2$. By abuse of notation, let $p(1)$ be the corresponding point in $E_1 \subset \mathbb{K}$. Likewise, the intersection of $\overline{\mathcal{O}'_1}$ with $\mathcal{L}_1^+$ is at the special point $\overline{p}(1)$ that is identified with the point $\overline{p}'(1) = (2, \theta_1, 2) \in L_1^+ \cap \{r = 2\}$. That is $\sigma_1(\overline{p}'(1)) = \overline{p}(1)$, $\tau(\overline{p}(1)) = \tau(\overline{p}'(1))$ and $r(\overline{p}'(1)) = 2$. By abuse of notation, let $\overline{p}(1)$ be the corresponding point in $S_1 \subset \mathbb{K}$.

In general, I will use the same notation for points in $\mathcal{L}_i^\pm$ and their images under τ in E_i and S_i for $i = 1, 2$. The corresponding points in $L_i^\pm$ are marked with a prime.

The positive $\mathcal{K}$-orbit of a point in $\tau(\mathcal{O}'_1)$ continues after crossing E_1 at $p(1)$ as a trapped $\mathcal{W}$-orbit in the cylinder $\{r = 2\}$, that is the image under τ of the $\mathcal{W}$-orbit of $p'(1)$. Since the $\mathcal{W}$-orbit of $p'(1)$ accumulates on $\mathcal{O}_1$, it intersects infinitely many times $\mathcal{L}_1^-$. Then the image under τ of this orbit intersects $E_1 = \tau(\mathcal{L}_1^-)$ infinitely many times. Let $p(1; 1, 1)$ be the first intersection. Denote by $p'(1; 1, 1) \in L_1^-$ the point in the entrance of $\mathbb{W}$ such that $\tau(p'(1; 1, 1)) = p(1; 1, 1)$, then the Radius Inequality (K8) implies that $r(p'(1; 1, 1)) > 2$.

We need the following important result (we refer to Propositions 6.5 and 6.7 of [P5]):

PROPOSITION 1.3.1. *Let x be a primary or secondary entry point with $r(x) > 2$, let $\overline{x}$ be the exit point facing x ($x \equiv \overline{x}$). Then $\overline{x}$ is in the same $\mathcal{K}$-orbit as x and the $\mathcal{K}$-orbit of x contains the ordered collection of $\mathcal{W}$-arcs in the $\mathcal{W}$-orbit of x' that are in $\mathbb{W}'$, where $\tau(x') = x$.*

The proposition implies that the $\mathcal{K}$-orbit $\mathcal{S}_1$ will make a (a priori) complicated trajectory from $p(1; 1, 1) \in E_1 \subset \mathbb{K}$ before reaching S_1 at the facing point $\overline{p}(1; 1, 1)$ (this point is not necessarily the first intersection of the orbit with the secondary exit region S_1). Condition (K4) implies that $p(1; 1, 1)$ and $\overline{p}(1; 1, 1)$ belong to the same Wilson orbit that is contained in the cylinder $\{r = 2\}$.

The above description can be applied repeatedly to $\mathcal{S}_1$, always in the positive direction. From $\overline{p}(1; 1, 1)$ the orbit makes a turn around the cylinder $\{r = 2\}$ and intersects E_1 at a point $p(1; 1, 2)$ that is above $p(1; 1, 1)$ and below $p(1)$, as illustrated in Figure 1.23. Since $r(p(1; 1, 2)) > 2$, Proposition 1.3.1 applies once more implying that $\overline{p}(1; 1, 2) \in S_1$ facing $p(1; 1, 2)$ belongs to the orbit $\mathcal{S}_1$. We can then continue forever: from $\overline{p}(1; 1, 2)$ follows a $\mathcal{W}$-arc that makes a turn around the cylinder $\{r = 2\}$ to a point $p(1; 1, 3) \in E_1$, with $r(p(1; 1, 3)) > 2$. Then Proposition 1.3.1 guarantees that $\overline{p}(1; 1, 3) \in S_1$ is in $\mathcal{S}_1$, etc.

Since the $\mathcal{W}$-orbit of $p'(1)$ accumulates on the periodic orbit $\mathcal{O}_1$, the forward $\mathcal{K}$-orbit of $p(1) \in E_1 \subset \mathbb{K}$ accumulates on $\tau(\mathcal{O}'_1) \subset \mathcal{S}_1$. That is, recursively we obtain points $p(1; 1, \ell)$ for $\ell \geq 1$ in E_1 that belong to the special orbit $\mathcal{S}_1$ and accumulate on $p(1)$. The Radius Inequality (K8) implies that $r(p(1; 1, \ell))$ is an decreasing sequence converging to 2 as $\ell \to \infty$ (at least for ℓ big enough the sequence is decreasing).

REMARK 1.3.2. *We have obtained that the ω-limit of the points in $\mathcal{S}_1$, denoted by $\omega(\mathcal{S}_1)$, contains $\mathcal{O}'_1$ and thus contains $\mathcal{S}_1$. In other words, $\mathcal{S}_1 \subset \omega(\mathcal{S}_1)$.*

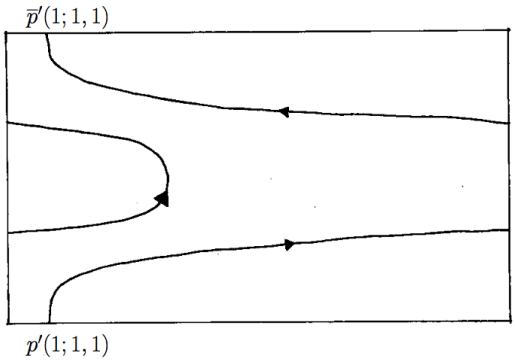

Figure 1.12: The intersection of the orbit of $p'(1;1,1)$ with the cylinder $\{r = r_1\}$

Now let us fill the gap between $p(1;1,1)$ and $\overline{p}(1;1,1)$, the same explanation applies to the segments of orbit between $p(1;1,\ell)$ and $\overline{p}(1;1,\ell)$ but gets increasingly complicated as ℓ grows since the radius of the starting point $p(1;1,\ell)$ is closer to 2. I will give an explanation for ℓ equal to 1 and 2.

As entry point $p(1;1,1)$ has radius greater than 2, thus the point $p'(1;1,1) \in L_1^- \subset \mathbb{W}$ has radius r_1 greater than 2. We have two possibilities, either the cylinder $\{r = r_1\}$ intersects the insertions or it does not. Assume that it does not as in Figure 1.12. Then the entire Wilson orbit of $p'(1;1,1)$ is contained in $\mathbb{W}'$ and hence the image under τ of the $\mathcal{W}$-orbit of $p'(1;1,1)$ is a segment of $\mathcal{K}$-orbit joining $p(1;1,1) \in E_1$ to $\overline{p}(1;1,1) \in S_1$.

From $\overline{p}(1;1,1)$ the orbit $\mathcal{S}_1$ makes one turn around the cylinder $\{r = 2\}$ and it intersects E_1 at the point $p(1;1,2)$. Proposition 1.3.1 implies that $\overline{p}(1;1,2) \in S_1$ belongs to the orbit $\mathcal{S}_1$. I will now explain how to fill the gap between these two points. The Radius Inequality (K8) implies that $r_2 = r(p(1;1,2)) > 2$. We have the same two possibilities as above, either the cylinder $\{r = r_2\}$ intersects the insertions or it does not (here I will assume that the insertions are symmetric in the sense that either the cylinder intersects both insertions or none). The latter case is the simple one as treated for $p(1;1,1)$. Now assume that the cylinder $\{r = r_2\}$ intersects both insertions and also that the $\mathcal{W}$-orbit of $p'(1;1,2)$ intersects both insertions, as in Figure 1.13.

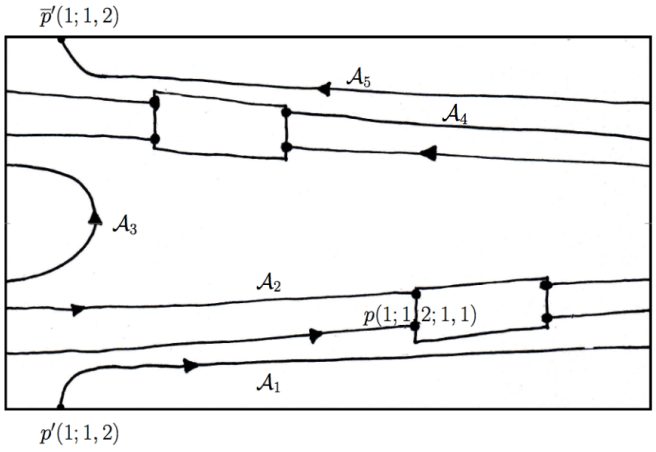

Figure 1.13: The intersection of the orbit of $p'(1;1,2)$ with the cylinder $\{r = r_2\}$

The intersection of the $\mathcal{W}$-orbit of $p'(1;1,2)$ with $\mathbb{W}'$ is a collection of $\mathcal{W}$-arcs between transition points, contained in the cylinder $\{r = r_2\}$. The second part of Proposition 1.3.1 means that the image under τ of all these arcs is contained in $\mathcal{S}_1$ and in the same order. Let us call these arcs $\mathcal{A}_j$ for $1 \leq j \leq n$ for some finite n (n is finite since the $\mathcal{W}$-orbit of $p'(1;1,2)$ is finite, in Figure 1.13 we have $n = 5$).

Clearly the image under τ of the arcs above does not completely fills the gap between $p(1;1,2)$ and $\overline{p}(1;1,2)$, since it is not a connected set. To do so, we need to understand what happens

between the endpoint of an arc $\mathcal{A}_j$ and the starting point of the following arc $\mathcal{A}_{j+1}$.

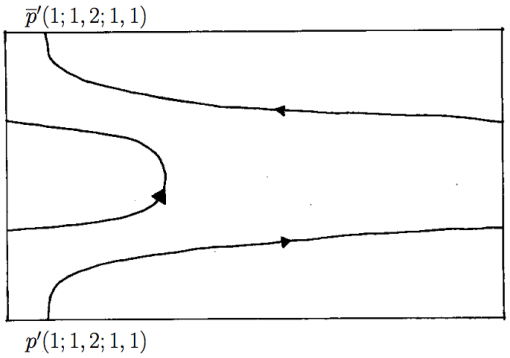

Figure 1.14: The intersection of the orbit of $p'(1;1,2;1,1)$ with the cylinder $\{r = r_{2,1}\}$

Let us follow the orbit from $p(1;1,2) = \tau(p'(1;1,2))$. We start by the image under τ of the first arc $\mathcal{A}_1$. The assumptions imply that the endpoint of this arc is a point in E_1 that we denote by $p(1;1,2;1,1)$. Let $p'(1;1,2;1,1) \in L_1^-$ be the corresponding point in the entrance of $\mathbb{W}$. Observe that the Radius Inequality (K8) implies that $r_2 < r_{2,1} = r(p(1;1,2;1,1))$. Again there are two possibilities: either the cylinder $\{r = r_{2,1}\}$ intersects the insertions or not. If not, the image under τ of the $\mathcal{W}$-orbit $p'(1;1,2;1,1)$ goes from $p(1;1,2;1,1)$ to the facing point $\overline{p}(1;1,2;1,1) \in S_1$ joining $\mathcal{A}_1$ to $\mathcal{A}_2$. If yes we have to iterate the description. Since each time that the orbit intersects a secondary entry point the radius grows, eventually it gets to a cylinder that does not intersects any of the insertions. So assume, to make the discussion shorter, that we are in the second case, as in Figure 1.14.

Recapitulating, under the assumptions made, we have

$$p(1;1,1) \xrightarrow{\tau(\mathcal{W}-\text{orbit})} \overline{p}(1;1,1) \xrightarrow{\mathcal{W}-\text{arc}} p(1;1,2) \xrightarrow{\tau(\mathcal{A}_1)} p(1;1,2;1,1) \xrightarrow{\tau(\mathcal{W}-\text{orbit})} \overline{p}(1;1,2;1,1),$$

where $\overline{p}(1;1,2;1,1) \in S_1$ is the starting point of the arc $\tau(\mathcal{A}_2)$ and it is facing $p(1;1,2;1,1)$ by condition (K4).

Now $\tau(\mathcal{A}_2)$ has its starting point in S_1 and its endpoint either in E_1 or in E_2 (in Figure 1.12 the endpoint of $\mathcal{A}_2$ is in $\mathcal{L}_1^-$ with $\tau(\mathcal{L}_1^-) = E_1$). Repeating the above description we fill in the orbit segment between the endpoint of $\tau(\mathcal{A}_2)$ and the starting point of $\tau(\mathcal{A}_3)$. We can thus join the collection of arcs $\tau(\mathcal{A}_j)$ and find the $\mathcal{K}$-orbit segment from $p(1;1,2)$ to $\overline{p}(1;1,2)$.

This finishes the description of the forward $\mathcal{K}$-orbit of points in $\mathcal{O}_1'$.

The above description applies without any significant changes to the backward orbit of $\mathcal{O}_1'$. Indeed the backward orbit of a point in $\mathcal{O}_1'$ intersects $\mathcal{L}_1^+$ in the special point $\overline{p}(1)$ facing $p(1)$ as in Figure 1.11. This point is identified with $\overline{p}'(1) \in L_1^+$ that has radius 2 and the intersection of the backward $\mathcal{W}$-orbit of this point with $\mathbb{W}'$ is mapped under τ to parts of $\mathcal{S}_1$. Since this $\mathcal{W}$-orbit accumulates in backward time on $\mathcal{O}_2$, then $\tau(\mathcal{O}_2')$ is contained in the α-limit of $\mathcal{S}_1$ and thus $\mathcal{S}_2 \subset \alpha(\mathcal{S}_1) \subset \overline{\mathcal{S}_1}$. Also, recursively, in the backward direction, we can fill the gaps to describe the entire orbit.

This is a first explanation of how the orbit $\mathcal{S}_1$ is *composed*. In the rest of this section, always add "the image under τ" to the sets considered. I will explain basically the same construction of $\mathcal{S}_1$, but in a new set of diagrams. For this we consider the level sets of $\mathcal{S}_1$. We need the following result (see Proposition 10.1 in [P5]).

PROPOSITION 1.3.3. *For $i = 1, 2$, there is a well-defined level function*

$$n_0 \colon \mathcal{S}_1 \cup \mathcal{S}_2 \to \mathbb{N} = \{0, 1, 2, \ldots\}, \tag{1.9}$$

such that $n_0^{-1}(0) = \tau(\mathcal{O}_1' \cup \mathcal{O}_2')$.

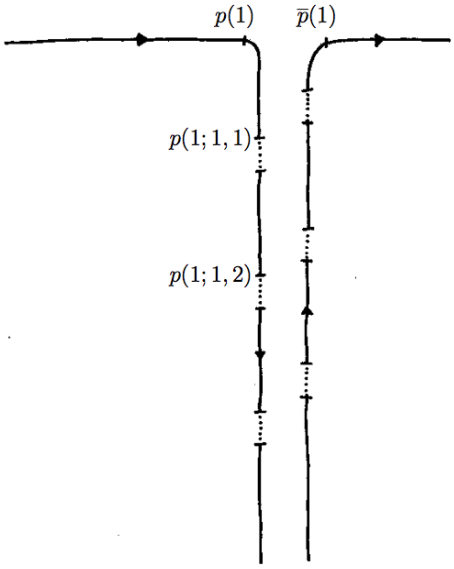

Figure 1.15: Level 0 and 1 of $\mathcal{S}_1$ with gaps

The level zero of $n_0|_{\mathcal{S}_1}$ is the arc $\tau(\mathcal{O}'_1)$ with endpoints $p(1)$ and $\overline{p}(1)$, represented by the horizontal segments in Figure 1.15. The level one is composed by (the image under τ of) two semi-infinite $\mathcal{W}$-orbits: the forward $\mathcal{W}$-orbit of $p'(1)$ and the backward $\mathcal{W}$-orbit of $\overline{p}'(1)$, represented by the two vertical lines in Figure 1.15. Observe that the vertical lines are not continuous: the dotted parts correspond to the arcs that are not in the intersection of these two $\mathcal{W}$-orbits with $\mathbb{W}'$. In other words, in the left-hand side vertical line the continuous segments correspond (from top to bottom) to the arcs from $p(1)$ to $p(1;1,1)$, from $\overline{p}(1;1,1)$ to $p(1;1,2)$, from $\overline{p}(1;1,2)$ to $p(1;1,3)$ and in general from $\overline{p}(1;1,\ell)$ to $p(1;1,\ell+1)$ for $\ell \geq 1$ and unbounded. The right-hand side vertical line is the backward orbit of $\overline{p}(1)$ that repeatedly intersects the second insertion.

Let me point out one aspect in this new set of flattened diagrams. In the plug $\mathbb{K}$ the left-hand side vertical continuous segments in Figure 1.15 correspond to arcs that accumulate on the horizontal segment $\tau(\mathcal{O}'_1)$, while the right-hand side vertical continuous segments accumulate on $\tau(\mathcal{O}'_2)$.

The level 2 of $\mathcal{S}_1$ is composed by all the finite $\mathcal{W}$-orbits starting at the intersections of the two level 1 orbits with E_1 and E_2. Thus by (the image under τ of) a countable collection of finite $\mathcal{W}$-orbits. Observe that since these are finite Wilson orbits, we just need to consider the starting

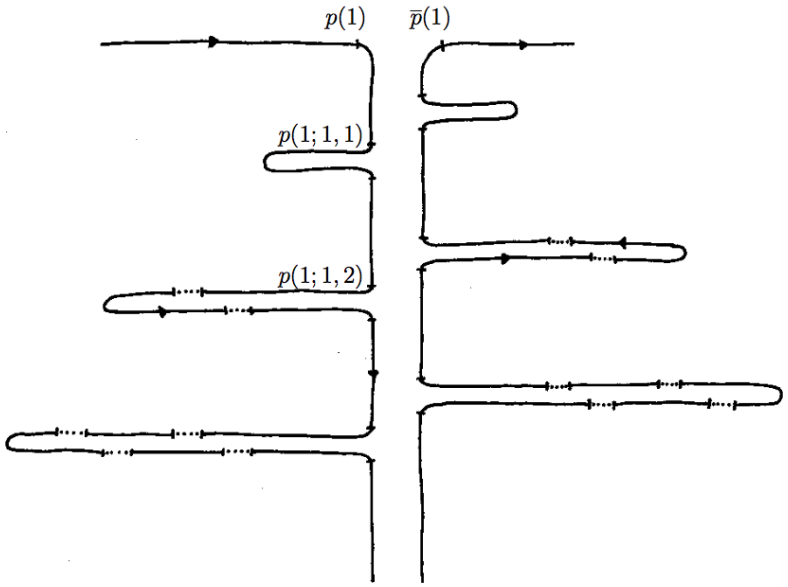

Figure 1.16: Level 0, 1 and 2 of $\mathcal{S}_1$ with gaps

point in the entrance of the insertions $E_1 \cup E_2$, Proposition 1.3.1 implies that they will contain the facing points in the exit of the insertions $S_1 \cup S_2$. I represent in Figure 1.16 these orbits as the border of horizontal tongues, because of their shape inside $\mathbb{W}$ (as in Figures 1.2 and 1.3). Again the dotted parts are the segments that are not in the intersection with $\mathbb{W}'$ and thus do not belong to $\mathcal{S}_1$. As we travel downwards along the two level one $\mathcal{W}$-orbits the tongues that appear at level 2 get longer, since the radius of their starting point gets closer to 2. This also implies that, eventually, the tongues intersect the insertions. In Figure 1.16 (and Figure 1.17 below), the assumption is that the $\mathcal{W}$-orbit of $p'(1;1,1)$ does not intersects the insertions and the $\mathcal{W}$-orbit of $p'(1;1,2)$ intersects both insertions. Then the intersection of the $\mathcal{W}$-orbit of $p'(1;1,2)$ with $\mathbb{W}'$ is composed of the arcs $\mathcal{A}_j$ for $1 \leq j \leq k$ and k finite. In Figure 1.16 the value of k is 3.

At any level n greater than 2, we consider the $\mathcal{W}$-orbits of the points in the intersection of the

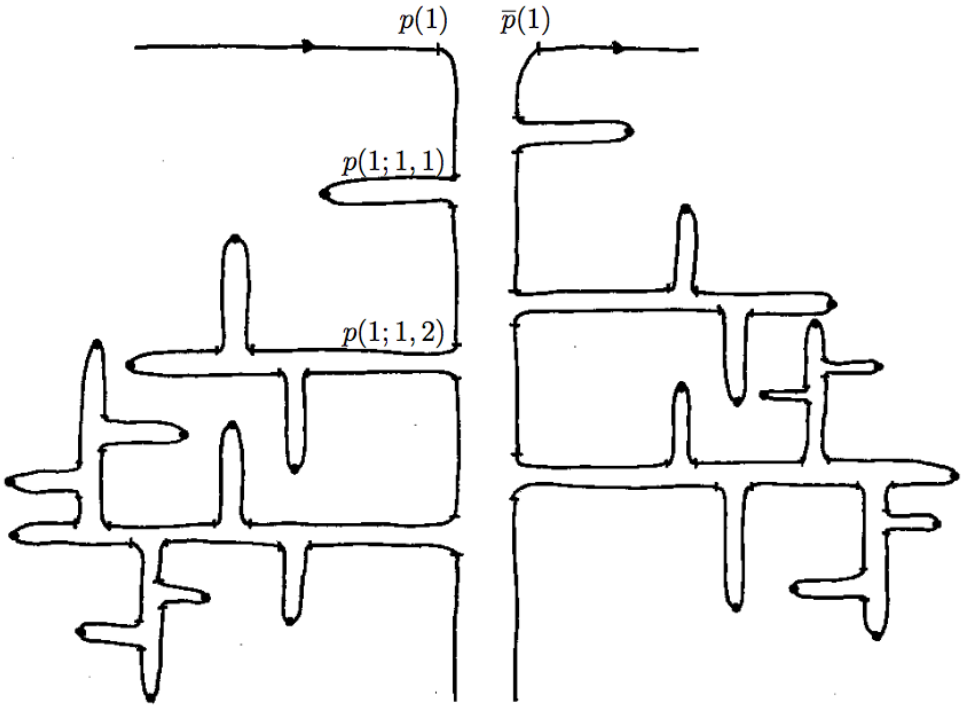

Figure 1.17: The tree diagram for $\mathcal{S}_1$ with marked tips

$\mathcal{W}$-orbits at level $n-1$ with the entry regions E_1 and E_2. Recursively we obtain the diagram, in Figure 1.17, representing levels 0 to 4. This situation repeats again at any level, adding to the complexity of the diagram in Figure 1.17.

Observe that this set of diagrams explain the concatenation of pieces of Wilson orbits that form the special orbit $\mathcal{S}_1$, but do not reflect how the orbit is embedded in $\mathbb{K}$. The embedding is quite complicated by the nature of the maps σ_i, for $i = 1, 2$. In particular, the width of the tongues that appear is roughly the same and equals the width of the Reeb cylinder, as a consequence of the shape of Wilson orbits. I will come back to this point in Section 1.3.2.

In Figure 1.17, I marked a set of points: every finite $\mathcal{W}$-orbit intersects the annulus $\{z = 0\}$ at a single point. Condition (W1) implies that at this point the vector field $\mathcal{W}$ is vertical and by condition (K3) this point is in $\mathbb{W}'$ (since all the finite Wilson orbits we are considering have radius greater than 2). For a finite $\mathcal{W}$-orbit we will call this point its tip.

Consider thus the set of tips contained in $\mathcal{S}_1$ and their lifts to $\mathbb{W}'$. We obtain a countable set

of points in the annulus $\{z = 0\}$, whose radii are arbitrarily close to 2. Hence the closed set $\overline{\mathcal{S}_1}$ contains points in $\tau(\mathcal{R}')$ the image of the Reeb cylinder in $\mathbb{K}$.

I finish this section pointing out some conclusions:

— $\mathcal{S}_i \subset \overline{\mathcal{S}_j}$ for all $i, j = 1, 2$, thus $\overline{\mathcal{S}_1} = \overline{\mathcal{S}_2} = \Sigma$ is the minimal set.

— Σ contains points in $\tau(\mathcal{R}')$.

We are faced with a dichotomy: either the tips in $\mathcal{S}_1 \cup \mathcal{S}_2$ accumulate on a Cantor set in the circle $\{z = 0, r = 2\}$ contained in $\tau(\mathcal{R}')$ or they accumulate on the whole circle. Theorem 17.1 in [P5] states that under the generic hypotheses (see Remark 1.2.1 and Section 1.6), the tips accumulate on the whole circle, implying that Σ has topological dimension 2. A description of this set, more precisely a dense dimension 2 subset of Σ is given in the following section. We do not know if there is a smooth Kuperberg plug for which the minimal set has dimension 1. In the piecewise linear category, G. Kuperberg and K. Kuperberg [KK96] construct a plug with a 1-dimensional minimal set.

1.3.2 $\mathfrak{M}_0$, a dense subset of the minimal set

In this section I describe a dense dimension 2 subset of Σ for a generic Kuperberg flow, that is denoted by $\mathfrak{M}_0$. The set $\mathfrak{M}_0$ is obtained by flowing inside $\mathbb{K}$ the notched Reeb cylinder $\tau(\mathcal{R}')$ and the description is very similar to the decomposition of $\mathcal{S}_1$ by levels explained in Figures 1.15, 1.16 and 1.17. Before starting, I need to introduce two types of surfaces in $\mathbb{W}$: finite and infinite propellers.

For a moment, we will work in the Wilson plug. Consider a curve γ in the entry region $\partial_h^- \mathbb{W}$ of the plug. We parametrize this curve as $\gamma(t)$ with $t \in [0, 1]$ and we assume that:

— $r(\gamma(0)) = 3$;

— $r(\gamma(1)) < r(\gamma(t))$ for $t \in [0, 1)$;

— $r(\gamma(1)) \geq 2$.

The propeller P_γ is obtained by flowing γ inside the Wilson plug. In the following figures we assume that γ is transverse to the cylinders $\{r = cst.\}$, just to make the figures simpler. I describe next the surface P_γ.

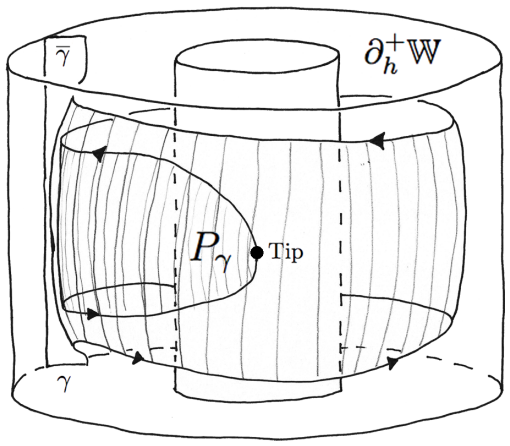

Figure 1.18: Finite propeller inside $\mathbb{W}$

If $r(\gamma(1)) > 2$ describing P_γ is a simple game. Indeed the $\mathcal{W}$-orbit of every point in γ is finite, as it exits the plug in some finite time. The finite propeller P_γ is the compact surface composed by the finite orbits of the points $\gamma(t)$ for $t \in [0, 1]$. It has the shape of a tongue that turns in the positive θ-direction as in Figure 1.18. Its boundary is composed by γ in the entry region of $\mathbb{W}$, the facing curve $\overline{\gamma}$ in the exit region of $\mathbb{W}$, the orbit of $\gamma(0)$ that is just a vertical segment in the vertical boundary of $\mathbb{W}$ and the orbit of $\gamma(1)$. Observe that the orbit of $\gamma(1)$ gets longer as the radius of $\gamma(1)$ tends to 2.

If $r(\gamma(1)) = 2$ it is not so simple since the forward orbit of $\gamma(1)$ is trapped. We consider in this case the forward orbits of the points in the curve γ and the backward orbits of the points in the facing curve $\overline{\gamma}$, for all times for which the orbits are defined. Equivalently, we consider the union of finite propellers P_{γ_s} for $s \in [0, 1)$ and $\gamma_s \subset \gamma$ the curve obtained as $\gamma([0, s])$ and the two semi-infinite orbits: the forward orbit of $\gamma(1)$ and the backward orbit of the facing point $\overline{\gamma}(1)$. The

infinite propeller P_γ is an open surface that turns infinitely many times around the Reeb cylinder $\mathcal{R}$. Observe that we do not consider its closure that consists of the union of P_γ and $\mathcal{R}$.

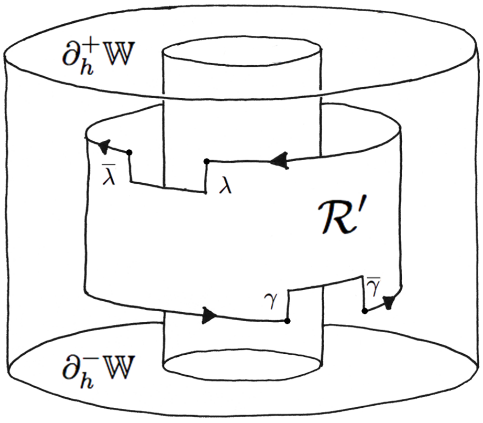

Figure 1.19: $\mathcal{R}' \subset \mathbb{W}$

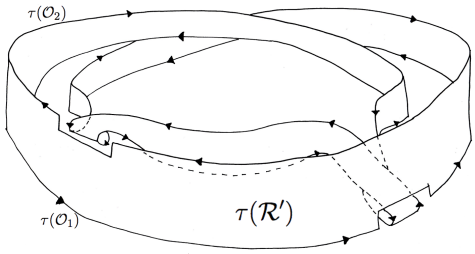

Figure 1.20: $\tau(\mathcal{R}') \subset \mathbb{K}$

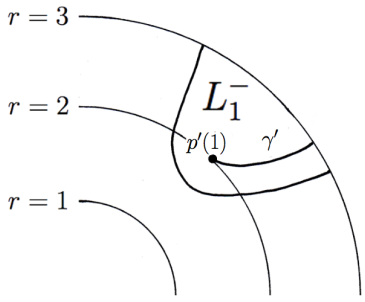

Figure 1.21: γ' in L_1^-

Propellers are the blocks to build the surface $\mathfrak{M}_0$ in the Kuperberg plug. To describe $\mathfrak{M}_0$ we divide it by levels, Proposition 10.1 from [P5] states:

PROPOSITION 1.3.4. *There is a well-defined level function*

$$n_0 \colon \mathfrak{M}_0 \to \mathbb{N} = \{0, 1, 2, \ldots\}, \tag{1.10}$$

such that $n_0^{-1}(0) = \tau(\mathcal{R}')$.

Let $\mathfrak{M}_0^k \subset \mathfrak{M}_0$ be the set of points at level at must k, I describe next these sets for $k = 0, 1, 2$.

The level zero set is the image under τ of the notched Reeb cylinder $\mathcal{R}' = \mathcal{R} \cap \mathbb{W}'$. In $\mathbb{W}'$ it is easy to visualize it (as in Figure 1.19), in $\mathbb{K}$ it is a little bit more difficult. Figure 1.20 is an attempt to represent this set as it is embedded in $\mathbb{K} \subset \mathbb{R}^3$. What the map σ_1 does to this cylinder is to choose a vertical segment in the cylinder ($\{\theta = \theta_1\}$ in condition (K7)) and turns it to make it tangent to part of the boundary of the cylinder that got erased by the lower notch. Analogously, σ_2 chooses a vertical segment in the cylinder ($\{\theta = \theta_2\}$ in condition (K7)) and turns it to make it tangent to part of the boundary of the cylinder that got erased by the upper notch. The directions of the flow force the two turns to be in opposite directions.

Observe that $\mathcal{R}' \cap \mathcal{L}_1^-$ is a vertical line that we call the curve γ (as in Figure 1.19) and let γ' be the corresponding curve in L_1^- (as in Figure 1.21). That is $\sigma_1(\gamma') = \gamma$ and $\tau(\gamma') = \tau(\gamma)$. Analogously we have a curve $\lambda \in \mathcal{L}_2^-$ and $\lambda' \in L_2^-$.

Since L_1^- and L_2^- are subsets of the entry region of $\mathbb{W}$, consider the two infinite propellers $P_\gamma \subset \mathbb{W}$ generated by the curve γ' and P_λ generated by λ' in $\mathbb{W}$. The set $\mathfrak{M}_0^1$ of points with level at most one consists of the image under τ of the Reeb cylinder and the two infinite propellers P_γ and P_λ. Each of these propellers intersects infinitely many times the insertions, thus $P'_\gamma = P_\gamma \cap \mathbb{W}'$ and $P'_\lambda = P_\lambda \cap \mathbb{W}'$ have infinitely many notches each.

In analogy with Figure 1.15, Figure 1.22 is a flattened diagram of $\mathfrak{M}_0^1$. The horizontal band is the notched Reeb cylinder $\mathcal{R}'$, whose lower boundary is $\mathcal{O}'_1$ and whose upper boundary is $\mathcal{O}'_2$, union the boundaries of the notches. The two vertical bands correspond to P'_γ (the lower one) and P'_λ (the upper one), parts of their boundaries are contained in $\mathcal{S}_1$ and $\mathcal{S}_2$ respectively. The set $\mathfrak{M}_0^1$

in $\mathbb{K}$ is embedded differently, since the two infinite propellers turn around the Reeb cylinder that is itself embedded as in Figure 1.20. I wont attempt to draw an image of this.

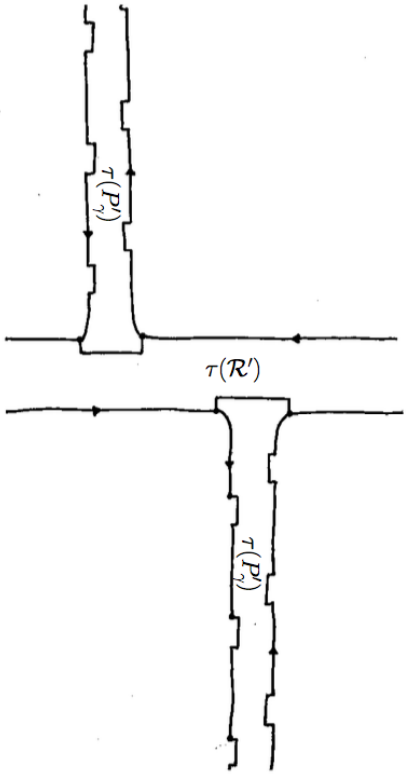

Figure 1.22: Flattened $\mathfrak{M}_0^1$

The set $\mathfrak{M}_0^2$ consists of $\mathfrak{M}_0^1$ union the image under τ of a countable set of finite propellers. Indeed each notch in P'_γ or P'_λ has to be filled with a propeller. The intersection of $\tau(P'_\gamma)$ with E_i for $i = 1, 2$ consist of a countable family of curves, that by the Radius Inequality (K8) are contained in the set $\{r > 2\}$. Each one of these curves in E_1 corresponds to a point $p(1; 1, \ell)$ for $\ell \geq 1$ and unbounded. The first two curves are illustrated in Figure 1.23. Each curve in E_i is mapped under σ_i^{-1} to a curve in L_i^-, for $i = 1, 2$, that generates a finite propeller in $\mathbb{W}$. The image under τ of these finite propellers is contained in $\mathfrak{M}_0^2$. Analogously for $\tau(P'_\lambda)$. Each of these propellers adds a finite tongue to Figure 1.22, that gets longer as we travel along the level one infinite propellers $\tau(P'_\gamma)$ and $\tau(P'_\lambda)$. The finite propellers might have notches, since if they are long enough they will intersect the insertions. The tongues at level 1 are the horizontal tongues attached to the flattened infinite propellers in Figure 1.24 (where just $\tau(P'_\gamma)$ and some of its ramifications are illustrated, the upper side corresponding to $\tau(P'_\lambda)$ is analogous).

The level three set $\mathfrak{M}_0^3$ is obtained from $\mathfrak{M}_0^2$ by filling the notches of the level 2 propellers with finite propellers. Analogously $\mathfrak{M}_0^k$ is obtained from $\mathfrak{M}_0^{k-1}$ by filling the notches of the level $k-1$ propellers with finite propellers. This process continues and gives the surface $\mathfrak{M}_0$.

Under the generic hypotheses, the closure of $\mathfrak{M}_0$ is the minimal set Σ. This means that the "boundary" of $\mathfrak{M}_0$ that consists of the orbits $\mathcal{S}_1$ and $\mathcal{S}_2$ is dense in $\mathfrak{M}_0$. In Chapter 18 of [P5] we prove that $\Sigma = \overline{\mathfrak{M}_0}$ is a zippered lamination, roughly meaning that the interior has the structure of a lamination (transversely Cantor) and the boundary is dense in the interior of the leaves. The definitions of interior and boundary for Σ are made precise in [P5]. I summarize the description in the last two sections with the following statement.

THEOREM 1.3.5 (Theorems 17.1 and 19.1 of [P5]). *For a generic Kuperberg flow $\overline{\mathfrak{M}_0} = \Sigma$ is the minimal set of the plug. The set Σ has topological dimension 2 and contains:*

— *an open 2-dimensional subset that forms a lamination with open leaves;*

— *a 1-dimensional subset that is dense in the previous set.*

These two sets are disjoint.

Let me say a few words about the theorem. The lamination contains the interior of $\mathfrak{M}_0$, obtained by flowing the open notched Reeb cylinder, thus $\mathfrak{M}_0$ minus the two special orbits. But $\mathfrak{M}_0$ is not transversely a Cantor set, while the lamination in Theorem 1.3.5 is. In Chapters 18 and 19 of [P5] we study the intersection of $\mathfrak{M}_0$ with a rectangle $\{\theta = cst.\}$, as the rectangle $\mathbf{R}_0$ introduced in the

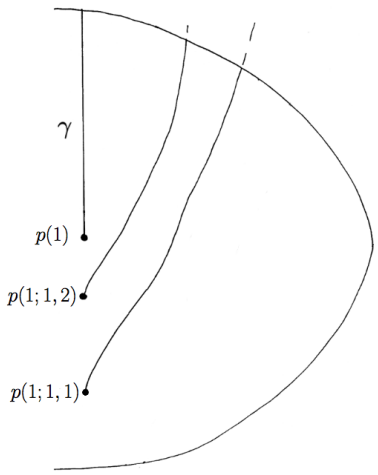

Figure 1.23: Curves in $\tau(P'_\gamma) \cap E_1$

following section. This allows to understand the intersection of $\Sigma \setminus \mathfrak{M}_0$ with a given rectangle and describe the lamination in the theorem. Consider the rectangles $\{\theta = cst.\}$ that do not intersect the insertions. Recall that each one of these rectangles has coordinates $r \in [1,3]$ and $z \in [-2,2]$. The intersection of Σ with each rectangle is a set symmetric with respect to the line $\{z = 0\}$ and formed by three types of sets:

1. a set of closed curves that is at most countable;
2. a set of points (that contains the tips of propellers);
3. a set of closed arcs (of uniformly bounded length).

The last two sets are not countable. The first set and the interior of the arcs in the third set are the intersection of the lamination in Theorem 1.3.5 with the rectangle, while the second set and the endpoints of the arcs in the third set are the intersection of the 1-dimensional subset in Theorem 1.3.5 with the rectangle.

REMARK 1.3.6. *Observe from Figure 1.24 that $\mathfrak{M}_0$ has the structure of a tree whose branches correspond to the propellers and can be rooted by the choice of a point in $\tau(\mathcal{R}')$. The growth of this tree is then the growth of the leaves in the lamination of Theorem 1.3.5 and is studied in Chapter 14 of [P5]. The growth is closely related to the growth of words in the* pseudo⋆group $\mathcal{G}^*_K$*, introduced in the following section.*

1.4 Pseudogroups

A tool introduced in [P5] that is used to study the dynamics of the flow, are the pseudogroups and pseudo⋆group acting on an almost transverse rectangle. In a pseudo⋆group we consider only compositions of a (symmetric) generating set, but we do not ask for the condition on union of maps to be in the pseudo⋆group, as for pseudogroups. This section corresponds to parts of Chapter 9 of [P5], where all details and proofs can be consulted. I introduce here the main maps, that arise in the discussions in Sections 1.4.2 and 1.5 related to entropy.

In the plugs $\mathbb{W}$ and $\mathbb{K}$ we can consider the rectangles $\{\theta = cst.\}$, one of them in $\mathbb{K}$ is depicted in Figure 1.25.

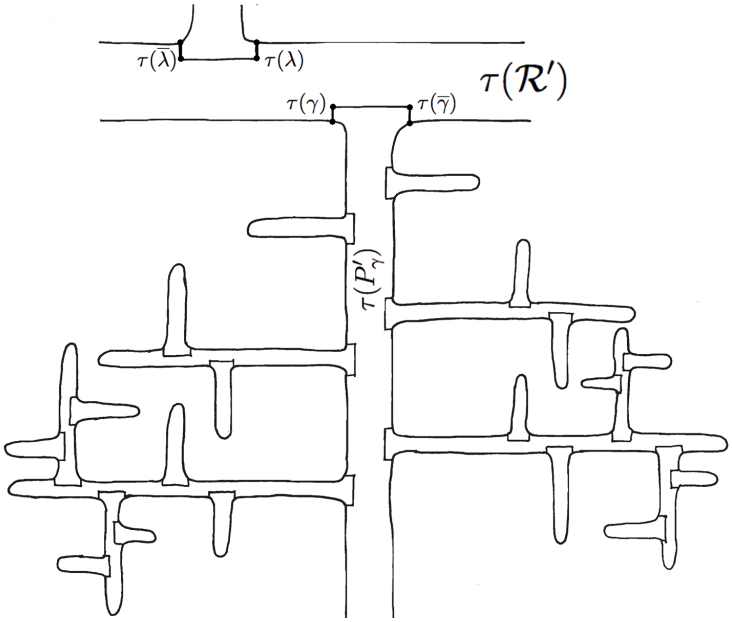

Figure 1.24: Flattened $\mathfrak{M}_0$

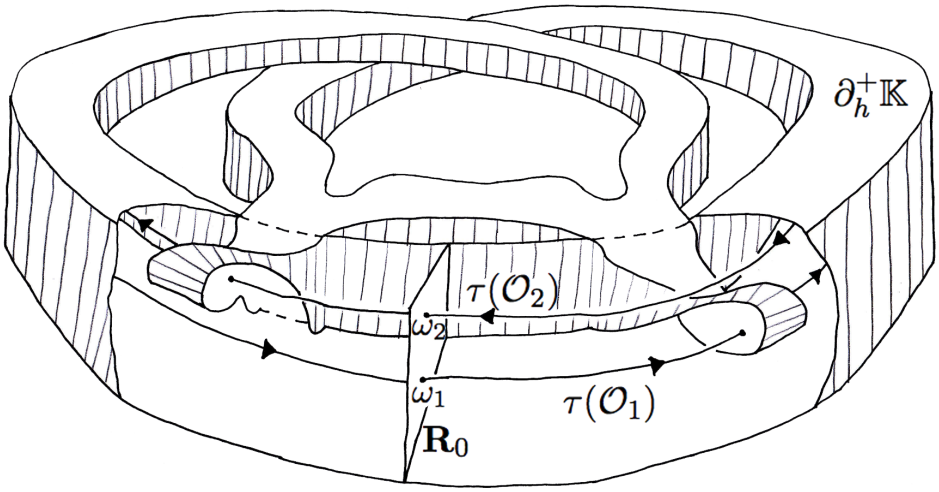

Figure 1.25: A rectangle $\mathbf{R}_0$ in the Kuperberg Plug $\mathbb{K}$

We must be careful to chose a value θ_0 so that the rectangle $\mathbf{R}_0 = \{\theta = \theta_0\} \subset \mathbb{W}$ does not intersect neither D_i nor $\mathcal{D}_i$ for $i = 1$ and 2. Let $\mathbf{R}_0$ be the corresponding rectangle in $\mathbb{K}$, we use the same notation since τ is bijective when restricted to such a rectangle. I will ask one more thing to this rectangle, that it lies between the two insertions as in Figure 1.25, so that from the upper part ($z > 0$) points flow to the upper insertion and from the bottom part ($z < 0$) points flow to the lower insertion.

Observe that, either in $\mathbb{W}$ or in $\mathbb{K}$, the vector field is tangent to the rectangle near the boundary and also at the line $\{z = 0\}$. Let $\omega_i \in \mathbf{R}_0$ be the intersection of the periodic orbit $\mathcal{O}_i$ with $\mathbf{R}_0$ when considering the rectangle in $\mathbb{W}$ or the intersection of the arc $\mathcal{O}'_i$ with $\mathbf{R}_0$ when considering the rectangle in $\mathbb{K}$, for $i = 1, 2$.

A finite $\mathcal{W}$-orbit, that is an orbit going from the entrance to the exit of the plug $\mathbb{W}$, if it intersects $\mathbf{R}_0$, it does so in a symmetric pattern with respect to the line $\{z = 0\}$. In this case, the construction of the flow implies that the intersection consists of a finite sequence of points contained in the vertical line of constant radius (the value of the radius is determined by the orbit). We have to consider two situations, either the orbit is tangent to $\mathbf{R}_0$ at the line $\{z = 0\}$ or not, in both situations the points in the intersection of the orbit with $\mathbf{R}_0$ are paired: for each point $(r, -z)$ in the intersection, (r, z) is also in the intersection.

We can define a first return map $\widehat{\Psi}$ for the flow Ψ_t, that will have discontinuities (I refer to Chapter 9 of [P5] for a complete discussion of the discontinuities and other properties of this map). The domain of $\widehat{\Psi}$ is the set:

$$Dom(\widehat{\Psi}) = \{\xi \in \mathbf{R}_0 \mid \exists\ t > 0 \ \text{ such that } \Psi_t(\xi) \in \mathbf{R}_0 \text{ and } \Psi_s(\xi) \notin \mathbf{R}_0 \text{ for } 0 < s < t\}\,. \quad (1.11)$$

The radius function is constant along the orbits of the Wilson flow, so that $r(\widehat{\Psi}(\xi)) = r(\xi)$ for all $\xi \in Dom(\widehat{\Psi})$. Also, note that the points ω_i for $i = 1, 2$ are fixed-points for $\widehat{\Psi}$ and for all other points $\xi \in \mathbf{R}_0$ with $\xi \neq \omega_i$, points climb up that is $z(\widehat{\Psi}(\xi)) > z(\xi)$.

Here I will consider just two types of first return maps for the flow Φ_t, instead of considering the general first return map that is too complicated for a succinct discussion. Observe first that if an arc of $\mathcal{K}$-orbit $[\xi, \eta]_{\mathcal{K}}$ with ξ and η in $\mathbf{R}_0$ does not contains transition points and its intersection with $\mathbf{R}_0$ is only at its endpoints, then $\eta = \widehat{\Psi}(\xi)$. For $i = 1, 2$, let $U_{\phi_i^+} \subset \mathbf{R}_0$ be the subset consisting of points ξ such that the $\mathcal{K}$-arc $[\xi, \eta]_{\mathcal{K}}$ contains a single transition point $x \in E_i$ and its intersection with $\mathbf{R}_0$ is only at the endpoints ξ and η. Note that for such ξ, we see from Figures 1.10 and 1.25, that its $\mathcal{K}$-orbit exits the surface E_i as the $\mathcal{W}$-orbit of a point $x' \in L_i^-$ with $\tau(x') = x \in E_i$, flowing upwards from $\partial_h^- \mathbb{W}$ until it intersects $\mathbf{R}_0$ again. If the $\mathcal{K}$-orbit of ξ enters E_i but exits through S_i before crossing $\mathbf{R}_0$, then ξ is not considered to be in the set $U_{\phi_i^+}$, since its orbits contains more than one transition point before returning to $\mathbf{R}_0$. Let $\phi_i^+ \colon U_{\phi_i^+} \to V_{\phi_i^+}$. As the $\mathcal{K}$-arcs $[\xi, \eta]_{\mathcal{K}}$ defining ϕ_i^+ do not intersect $\mathcal{A}$, the restricted map ϕ_i^+ is continuous. The sets $U_{\phi_i^+}$ and $V_{\phi_i^+}$ are sketched in the left-hand side illustration in Figure 1.26.

For $i = 1, 2$, let $U_{\phi_i^-} \subset \mathbf{R}_0$ be the subset of $\mathbf{R}_0$ consisting of points ξ such that the $\mathcal{K}$-arc $[\xi, \eta]_{\mathcal{K}}$ contains a single transition point $x \in S_i$ and its intersection with $\mathbf{R}_0$ is only at the endpoints ξ and η. Then let $\phi_i^- \colon U_{\phi_i^-} \to V_{\phi_i^-}$. Again, as the $\mathcal{K}$-arcs $[\xi, \eta]_{\mathcal{K}}$ defining the maps ϕ_i^- do not intersect $\mathcal{A}$, the restricted map ϕ_i^- is continuous. The sets $U_{\phi_i^-}$ and $V_{\phi_i^-}$ are sketched in the right-hand side illustration in Figure 1.26.

Let me comment on some details of the regions in Figures 1.26 (a) and (b). For the map ϕ_i^+, $i = 1, 2$, the domain contains a neighborhood of the point ω_i. Flowing the domain $U_{\phi_i^+}$ forward to E_i and then applying the map σ_i^{-1} we obtain a set $\widetilde{U_{\phi_i^+}} \subset L_i^-$ containing points with r-coordinate equal to 2. Observe that the Radius Inequality implies that the maximum radius of points in $\widetilde{U_{\phi_i^+}}$ is bigger than the maximum radius of points in $U_{\phi_i^+}$. The first intersection of the $\mathcal{W}$-orbits of points

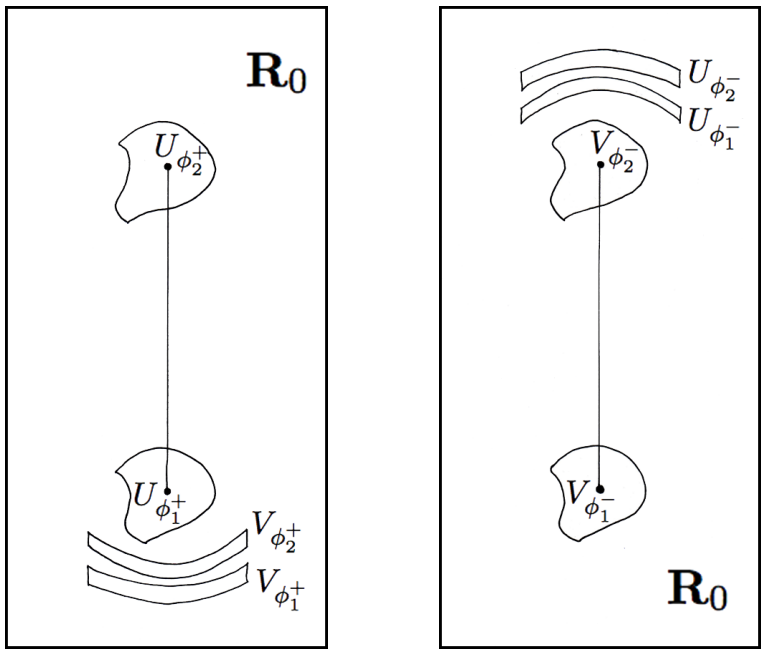

(a) Domains of ϕ_1^+, ϕ_2^+ (b) Domains of ϕ_1^-, ϕ_2^-

Figure 1.26: Domains and ranges for the maps $\{\phi_1^+, \phi_2^+, \phi_1^-, \phi_2^-\}$

in $\widetilde{U_{\phi_i^+}}$ with $\mathbf{R}_0$ is thus a region containing points with r-coordinate equal to 2 and since these points climb slower than other points, the region folds at $\{r = 2\}$. Similar considerations apply to the maps ϕ_i^- for $i = 1, 2$.

Observe that each map ϕ_i^+ for $i = 1, 2$ corresponds to a flow through a transition point which increases the level function $n_x(t)$ by $+1$, so the inverse of ϕ_i^+ decreases the level function by -1. The map ϕ_i^- decreases the level by -1 and its inverse increases the level by $+1$.

Next, define the subset of $\mathbf{R}_0$ contained in the domain of the Wilson map $\widehat{\Psi}$:

$$\mathbf{R}_0^* \quad = \quad \{(r, \theta_0, z) \in Dom(\widehat{\Psi}) \mid r \geq 2\} \setminus \{\omega_1, \omega_2\}$$

Proposition 1.3.1 implies (but it is not completely trivial) that there is a subset U_ψ of $\mathbf{R}_0$ that contains $\mathbf{R}_0^*$ such that the restriction of $\widehat{\Psi}$ to U_ψ is a map representing part of the dynamics of the Kuperberg flow: if $\widehat{\Phi}$ is the first return map to $\mathbf{R}_0$ of the Kuperberg flow, then $\psi = \widehat{\Psi}|_{U_\psi}$ is a power of $\widehat{\Phi}$ (I refer to Lemma 9.6 in [P5]).

We have five special elements $\{\phi_1^+, \phi_1^-, \phi_2^+, \phi_2^-, \psi\}$ acting on subsets of $\mathbf{R}_0$, each of which reflects aspects of the dynamics of the flow Φ_t.

DEFINITION 1.4.1. *Let $\mathcal{G}_K^*$ denote the collection of all maps formed by compositions of the maps $\{Id, \phi_1^+, \phi_1^-, \phi_2^+, \phi_2^-, \psi\}$ and their restrictions to open subsets in their domains.*

Note that $\mathcal{G}_K^*$ is not necessarily a pseudogroup since it might not be true that $\phi : U \to V$ is a homeomorphism in $\mathcal{G}_K^*$ whenever there is a cover of U by open sets $\{U_a\}_{a \in I}$ such that $\phi|_{U_a} \in \mathcal{G}_K^*$ for all $a \in I$. The reason for not imposing this condition, is that many dynamical properties for flows admit corresponding versions for local maps defined by compositions of maps in this generating set, but not if we allow for arbitrary unions as for pseudogroups.

The importance of $\mathcal{G}_K^*$ is that its orbits are syndetic in the orbits of the flow. In [P5] this property is used to estimate the growth of the tree-like surface $\mathfrak{M}_0$ (Figure 1.24), give explicit computations for the entropy of the flow and the laminated entropy of the lamination in Theorem 1.3.5 (I refer to Chapters 14, 20, 21 and 22 of [P5]).

1.4.1 Shape of the minimal set

In this section, I present results in [P5] regarding topological properties of the minimal set Σ for a generic Kuperberg flow. The space Σ is compact and connected, so is a continuum. The natural framework for the study of topological properties of spaces such as Σ is using shape theory. For example, Krystyna Kuperberg posed the question whether Σ has stable shape? Stable shape is defined below and is about the nicest property one can expect for an exceptional minimal set. Theorem 1.4.5 below shows that Σ does not have stable shape. The proof of this result follows from the equality $\Sigma = \overline{\mathfrak{M}_0}$ for a generic Kuperberg flow and the structure theory developed in Section 1.3.2. It is a constructive proof: we describe in Chapter 23 of [P5] a system of generators for the first homology groups of a shape approximation (an example of such a generator is illustrated in Figure 1.27).

Shape theory studies the topological properties of a topological space $\mathfrak{Z}$ using a form of Čech homology theory. The definition of shape for a space $\mathfrak{Z}$ embedded in the Hilbert cube was introduced by Borsuk [Bor68, Bor75]. We give a brief definition of the shape of a compactum $\mathfrak{Z}$ embedded in a metric space X, following the work of Mardešić and Segal [MS82].

DEFINITION 1.4.2. *A sequence $\mathfrak{U} = \{U_\ell \mid \ell = 1, 2, \ldots\}$ is called a* shape approximation *of $\mathfrak{Z} \subset X$ if:*

1. *each U_ℓ is an open neighborhood of $\mathfrak{Z}$ in X which is homotopy equivalent to a compact polyhedron;*
2. *$U_{\ell+1} \subset U_\ell$ for $\ell \geq 1$ and their closures satisfy $\bigcap_{\ell \geq 1} \overline{U}_\ell = \mathfrak{Z}$.*

Suppose that X, X' are connected manifolds, that $\mathfrak{U}$ is a shape approximation for the compact subset $\mathfrak{Z} \subset X$ and $\mathfrak{U}'$ is a shape approximation for the compact subset $\mathfrak{Z}' \subset X'$. The compacta $\mathfrak{Z}, \mathfrak{Z}'$ are said to have the same shape if the following conditions are satisfied:

1. There is an order-preserving map $\phi\colon \mathbb{Z} \to \mathbb{Z}$ and for each $n \geq 1$ a continuous map $f_n\colon U_{\phi(n)} \to U'_n$ such that for any pair $n \leq m$, the restriction $f_n | U_{\phi(m)}$ is homotopic to f_m as maps from $U_{\phi(m)}$ to U'_n.

2. There is an order-preserving map $\psi\colon \mathbb{Z} \to \mathbb{Z}$ and for each $n \geq 1$ a continuous map $g_n\colon U'_{\psi(n)} \to U_n$ such that for any pair $n \leq m$, the restriction $g_n | U'_{\psi(m)}$ is homotopic to g_m as maps from $U'_{\psi(m)}$ to U_n.

3. For each $n \geq 1$, there exists $m \geq \max\{n, \phi \circ \psi(n)\}$ such that the restriction of $g_n \circ f_{\psi(n)}$ to U_m is homotopic to the inclusion as maps from U_m to U_n.

4. For each $n \geq 1$, there exists $m \geq \max\{n, \psi \circ \phi(n)\}$ such that the restriction of $f_n \circ g_{\phi(n)}$ to U'_m is homotopic to the inclusion as maps from U'_m to U'_n.

DEFINITION 1.4.3. *Let $\mathfrak{Z} \subset X$ be a compact subset of a connected manifold X. Then the* shape *of $\mathfrak{Z}$ is defined to be the equivalence class of a shape approximation of $\mathfrak{Z}$ as above.*

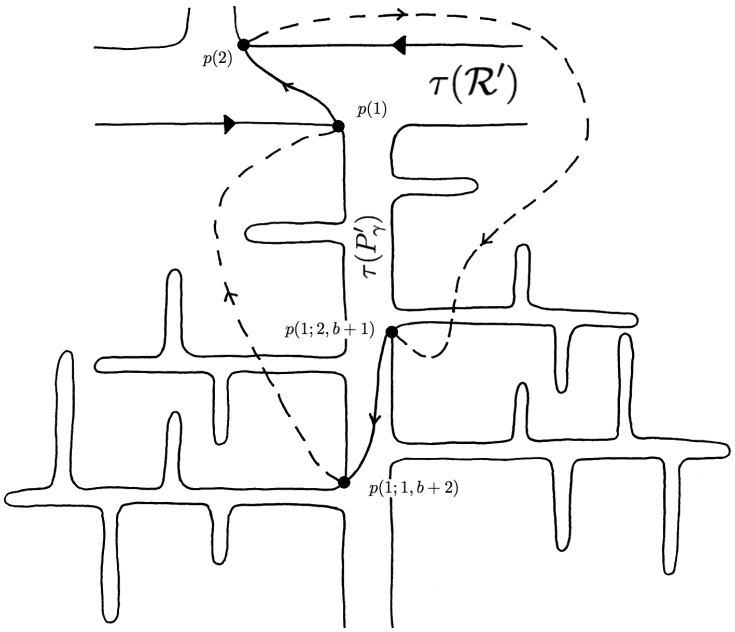

Figure 1.27: A pseudo-orbit as generator of the homology of the shape approximation

It is a basic fact of shape theory that this definition does not depend upon the choice of shape approximations and that two homotopic compacta have the same shape.

DEFINITION 1.4.4. *A compactum* $\mathfrak{Z}$ *has* stable shape *if it is* shape equivalent *to a finite polyhedron. That is, there exists a shape approximation* $\mathfrak{U}$ *such that each inclusion* $\iota\colon U_{\ell+1} \hookrightarrow U_\ell$ *induces a homotopy equivalence and* U_1 *has the homotopy type of a finite polyhedron.*

Some examples of spaces with stable shape are compact manifolds and more generally finite CW-complexes. A less obvious example is the minimal set for a Denjoy flow on $\mathbb{T}^2$ whose shape is equivalent to the wedge of two circles. In particular, the minimal sets of the aperiodic C^1-flow constructed by Schweitzer have stable shape, [Sch74]. The main result concerning generic Kuperberg flows is the following.

THEOREM 1.4.5. *The minimal set* Σ *of a generic Kuperberg flow does not have stable shape.*

Another important definition in shape theory is the following.

DEFINITION 1.4.6. *A compactum* $\mathfrak{Z} \subset X$ *is said to be* movable in X *if for every neighborhood* U *of* $\mathfrak{Z}$*, there exists a neighborhood* $U_0 \subset U$ *of* $\mathfrak{Z}$ *such that, for every neighborhood* $W \subset U_0$ *of* $\mathfrak{Z}$*, there is a continuous map* $\varphi\colon U_0 \times [0,1] \to U$ *satisfying the condition* $\varphi(x,0) = x$ *and* $\varphi(x,1) \in W$ *for every point* $x \in U_0$*.*

The notion of a movable compactum was introduced by Borsuk [Bor69], as a generalization of spaces having the shape of an *absolute neighborhood retract* (ANR's) and is an invariant of the shape of $\mathfrak{Z}$. It is a standard result that a compactum $\mathfrak{Z}$ with stable shape is movable. The movable property distinguishes between the shape of a Hawaiian earring and a Vietoris solenoid; the former is movable and the latter is not.

Showing the movable property for a space requires the construction of a homotopy retract φ with the properties stated in the definition, whose existence can be difficult to achieve in practice.

There is an alternate condition on homology groups, weaker than the movable condition, which is much easier to check.

PROPOSITION 1.4.7. *Let $\mathfrak{Z}$ be a movable compacta with shape approximation $\mathfrak{U}$. Then the homology groups satisfy the* Mittag-Leffler Condition*: For all $\ell \geq 1$, there exists $p \geq \ell$ such that for any $q \geq p$, the maps on homology groups for $m \geq 1$ induced by the inclusion maps satisfy*

$$Image\{H_m(U_p;\mathbb{Z}) \to H_m(U_\ell;\mathbb{Z})\} = Image\{H_m(U_q;\mathbb{Z}) \to H_m(U_\ell;\mathbb{Z})\} \ . \tag{1.12}$$

The above form of the Mittag-Leffler condition can be used to show that the Vietoris solenoid formed from the inverse limit of coverings of the circle is not movable.

I can now state an additional shape property for the minimal set of a generic Kuperberg flow.

THEOREM 1.4.8. *Let Σ be the minimal set for a generic Kuperberg flow. Then the Mittag-Leffler condition for homology groups is satisfied. That is, given a shape approximation $\mathfrak{U} = \{U_\ell\}$ for Σ, then for any $\ell \geq 1$ there exists $p > \ell$ such that for any $q \geq p$*

$$Image\{H_1(U_p;\mathbb{Z}) \to H_1(U_\ell;\mathbb{Z})\} = Image\{H_1(U_q;\mathbb{Z}) \to H_1(U_\ell;\mathbb{Z})\}. \tag{1.13}$$

The strategy for the proof of Theorem 1.4.5 is to construct a shape approximation $\mathfrak{U}$ for $\mathfrak{M}_0$ so that the conditions of Proposition 1.4.9 below are satisfied. This uses the properties of the level function n_0 defined in Proposition 1.3.4 and the double propellers introduced in Chapter 13 of [P5]. Double propellers provide a tool to build a set of neighborhoods of $\mathfrak{M}_0$ in which only propellers up to a certain fixed level can be distinguished. This provides a set of neighborhoods with sufficiently nice behavior so that we are able to exhibit a generating set of the first homology groups of the shape approximation, one is sketched in Figure 1.27 (the dotted curves represent small jumps in $E_1 \cup E_2 \cup S_1 \cup S_2$). The proof of Theorem 1.4.8 follows from the description of the homology groups.

PROPOSITION 1.4.9. *Let $\mathfrak{U} = \{U_\ell \mid \ell = 1, 2, \ldots\}$ be a shape approximation of $\mathfrak{Z} \subset X$, such that for $k > 0$*

— *the rank of $H_1(U_k;\mathbb{Z}) \geq 2^k$,*

— *for all $\ell > k$ the rank of the image $H_1(U_\ell;\mathbb{Z}) \to H_1(U_k;\mathbb{Z})$ is 3.*

Assume that for any shape approximation of $\mathfrak{V} = \{V_\ell \mid \ell = 1, 2, \ldots\}$ the rank of the homology groups $H_1(V_\ell;\mathbb{Z})$ is strictly greater than 3, then $\mathfrak{Z}$ does not have stable shape.

To finish this section I will state two conjectures, the first one about the minimal set of the Kuperberg plug and the second one about general minimal sets.

CONJECTURE 1.4.10. *For a generic Kuperberg flow the minimal set is movable.*

A proof needs a better description of the generators of the homology groups of a shape approximation. The second conjecture is motivated by the fact that the number of generators of the first homology groups of the shape approximation of $\mathfrak{M}_0$ proposed in [P5] grows exponentially with respect to the levels distinguished by the shape approximation and then also grows exponentially with respect to length. These generators are ϵ pseudo-orbits of the flow (that is pieces of orbits joined together by jumps of size bounded by ϵ).

CONJECTURE 1.4.11. *If an exceptional minimal set of a flow is not shape equivalent to a solenoid and has unstable shape, then the rank of the first homology groups of a shape approximation grows exponentially.*

In [BS90], the growth of the number of *separated* pseudo-orbits is related to the topological entropy of a flow. Thus if the conjecture is true and these generators can be interpreted as pseudo-orbits, a relation between shape and entropy type invariants could be explored.

1.4.2 Entropy of the minimal set

As mentioned in the introduction to this chapter, as a consequence of Katok's theorem on C^2-flows on 3-manifolds [Kat80], the topological entropy of a Kuperberg flow is zero. Indeed, Katok's theorem gives an upper bound of the topological entropy by the growth of the number of periodic orbits with respect to the period. Hence any aperiodic flow has topological entropy zero. In [P5] we use $\mathcal{G}_K^*$, introduced in Definition 1.4.1, to give an explicit computation of the topological entropy. This computation revealed chaotic behavior for the flow, but such that it evolves at a very slow rate and thus it does not result in positive topological entropy. We proved that, under some extra hypotheses, such generic Kuperberg flows have positive *slow entropy* and that the rates of chaotic behavior grow at a precise subexponential rate, as discussed in Chapter 21 of [P5].

To make the discussion more precise, let me give the definitions.

Define the entropy of the flow Φ_t using a variation of the Bowen formulation of topological entropy [Bow71] for a flow on a compact metric space (X, d_X). The definition we adopt is symmetric in the role of the time variable t. Two points $p, q \in X$ are said to be (φ_t, T, ϵ)-*separated* if

$$d_X(\varphi_t(p), \varphi_t(q)) > \epsilon \quad \text{for some} \quad -T \leq t \leq T \ .$$

A set $E \subset X$ is (φ_t, T, ϵ)-*separated* if all pairs of distinct points in E are (φ_t, T, ϵ)-separated. Let $s(\varphi_t, T, \epsilon)$ be the maximal cardinality of a (φ_t, T, ϵ)-separated set in X. Then the topological entropy is defined by

$$h_{top}(\varphi_t) = \frac{1}{2} \cdot \lim_{\epsilon \to 0} \left\{ \limsup_{T \to \infty} \frac{1}{T} \log(s(\varphi_t, T, \epsilon)) \right\}. \tag{1.14}$$

Moreover, for a compact space X, the entropy $h_{top}(\varphi_t)$ is independent of the choice of metric d_X.

A relative form of the topological entropy for a flow φ_t can be defined for any subset $Y \subset X$, by requiring that the collection of distinct (φ_t, T, ϵ)-separated points used in the definition (1.14) be contained in Y. The restricted topological entropy $h_{top}(\varphi_t | Y)$ is bounded above by $h_{top}(\varphi_t)$.

I recall now the definition of entropy for pseudo⋆groups as introduced by Ghys, Langevin and Walzcak in [GLW88]. Let (X, d_X) be a compact metric space and

$$\mathcal{G}_X^{(1)} = \{\varphi_0 = Id, \varphi_1, \varphi_1^{-1}, \ldots, \varphi_k, \varphi_k^{-1}\}$$

be a set of local homeomorphisms of X, with their inverses. Let $\mathcal{G}_X$ denote the pseudogroup generated by the collection of maps $\mathcal{G}_X^{(1)}$. Let $\mathcal{G}_X^* \subset \mathcal{G}_X$ denote the pseudo⋆group generated by the compositions of maps in $\mathcal{G}_X^{(1)}$ (as remarked after Definition 1.4.1, this might not be a pseudogroup). Let $\mathcal{G}_X^{(n)} \subset \mathcal{G}_X^*$ be the collection of maps defined by the restrictions of compositions of at most n elements of $\mathcal{G}_X^{(1)}$.

For $\epsilon > 0$, say that $x, y \in X$ are $(\mathcal{G}_X^*, n, \epsilon)$-*separated* if there exists $\varphi \in \mathcal{G}_X^{(n)}$ such that x, y are in the domain of φ and $d_X(\varphi(x), \varphi(y)) > \epsilon$. In particular, if the identity map is the only element of $\mathcal{G}_X^{(n)}$ which contains both x and y in its domain, then they are $(\mathcal{G}_X^*, n, \epsilon)$-separated if and only if $d_X(x, y) > \epsilon$. A finite set $E \subset X$ is said to be $(\mathcal{G}_X^*, n, \epsilon)$-*separated* if each distinct pair $x, y \in E$ is $(\mathcal{G}_X^*, n, \epsilon)$-separated. Let $s(\mathcal{G}_X^*, n, \epsilon)$ be the maximal cardinality of a $(\mathcal{G}_X^*, n, \epsilon)$-separated subset of X. Define the *entropy* of $\mathcal{G}_X^*$ by:

$$h_{GLW}(\mathcal{G}_X^*) \ = \ \lim_{\epsilon \to 0} \left\{ \limsup_{n \to \infty} \frac{1}{n} \ln(s(\mathcal{G}_X^*, n, \epsilon)) \right\}. \tag{1.15}$$

The property $0 < h_{GLW}(\mathcal{G}_X^*) < \infty$ is independent of the choice of metric on X.

The third entropy type invariant I want to introduce is the *slow entropy* of a map, first defined in the work of Katok and Thouvenot [KT97]. We adapted this idea for the action of a pseudo⋆group $\mathcal{G}_X^*$. For $0 < \alpha < 1$, define the α-entropy of $\mathcal{G}_X^*$, or just the slow entropy, by

$$h_{GLW}^{\alpha}(\mathcal{G}_X^*) \;=\; \lim_{\epsilon \to 0} \left\{ \limsup_{n \to \infty} \frac{1}{n^{\alpha}} \ln(s(\mathcal{G}_X^*, n, \epsilon)) \right\} \tag{1.16}$$

where $0 \leq h_{GLW}^{\alpha}(\mathcal{G}_X^*) \leq \infty$. If $h_{GLW}^{\alpha}(\mathcal{G}_X^*) > 0$ and $0 < \beta < \alpha$, then $h_{GLW}^{\beta}(\mathcal{G}_X^*) = \infty$. Analogously, one can define the slow entropy of a flow, by changing $1/T$ for $1/T^{\alpha}$ in (1.14).

The strategy in [P5] is to relate the flow entropy to the entropy of the pseudo⋆group $\mathcal{G}_K^*$. Estimating the entropy of $\mathcal{G}_K^*$ is equivalent to understanding how the tree $\mathfrak{M}_0$ grows (see Remark 1.3.6). This is done by estimating the number of admissible words in the generators $\{Id, \phi_1^+, \phi_1^-, \phi_2^+, \phi_2^-, \psi\}$ and their inverses (I refer to Chapter 14 in [P5]). We prove that, for a generic Kuperberg flow, the number of words is a subexponential function of the length and thus the entropy of $\mathcal{G}_K^*$ is zero.

The computation suggests that there are exponentially many separated points, but the time that the flow or the pseudo⋆group take to separate them is very long. We thus decided to study the slow-entropy of the holonomy pseudo⋆group of the lamination that we denote by $\mathcal{G}_{\mathfrak{M}}$. I won't go into the details here, but this pseudo⋆group is generated by $\{Id, \phi_1^+, \phi_2^+, \psi\}$ and their inverses. It turned out that to obtain that $h_{GLW}^{\alpha}(\mathcal{G}_{\mathfrak{M}}^*) > 0$ for $\alpha = 1/2$, we needed an extra hypothesis on the radius function defined by the insertions, that we baptized as *slow-growth*. Theorem 21.10 of [P5] states

THEOREM 1.4.12. *Let Φ_t be a generic Kuperberg flow. If the insertion maps σ_j have "slow growth", then $h_{GLW}^{1/2}(\mathcal{G}_{\mathfrak{M}}^*) > 0$.*

That the slow entropy of the lamination is positive implies (via a computation similar to the one carried out in Chapter 20 of [P5]), that the slow entropy of the flow Φ_t is positive. The words in the generators $\{Id, \phi_1^+, \phi_2^+, \psi\}$ used to prove Theorem 1.4.12 correspond to an exponentially growing family of loops that appear as generators of the first homology groups in the shape approximation used to prove Theorem 1.4.5. These two properties of Σ look very much a like. I wonder if there is a general relation between the shape of a minimal set and the (slow) entropy of the flow.

CONJECTURE 1.4.13. *Assume that a flow on a closed 3-manifold M has an exceptional minimal set Σ such that the rank of the first homology groups of a shape approximation grows exponentially, then the slow entropy of the flow is positive.*

1.5 Positive entropy in a C^{∞}-neighborhood of a generic Kuperberg plug

As remarked above, the topological entropy of a Kuperberg is zero, but the computations in [P5] revealed some chaotic behavior. In [P7] we study a C^{∞}-perturbation of a generic Kuperberg flow and we prove the following theorem.

THEOREM 1.5.1. *There exists a C^{∞} 1-parameter family of plugs $\mathbb{K}_{\epsilon}$ for $\epsilon \in (-1, a)$ for $a > 0$ such that:*

1. *The plug $\mathbb{K}_0$ is a generic Kuperberg plug;*
2. *For $\epsilon < 0$, the flow in the plug $\mathbb{K}_{\epsilon}$ has two periodic orbits that bound an invariant cylinder, every other orbit belongs to the wandering set and thus the flow has topological entropy zero;*

3. For $\epsilon > 0$, the flow in $\mathbb{K}_\epsilon$ has positive topological entropy and an abundance of periodic orbits.

The proof of Theorem 1.5.1 for $\epsilon < 0$ uses the same technical tools as developed in the previous works [Kup94, KK96, Ghys95, Mat95] for the study of the dynamics of the Kuperberg plug $\mathbb{K}_0$. The proof for $\epsilon > 0$ uses in a fundamental way the technique of relating the dynamics of a Kuperberg-like flow to the dynamics of its return map to an almost transverse rectangle, by introducing suitable pseudogroups as in Section 1.4.

I will not go into the details of the proof, but I explain the construction of the plugs $\mathbb{K}_\epsilon$ and give the main ideas to understand their dynamics. These plugs are constructed exactly as $\mathbb{K}$ in Section 1.2.1 except that conditions (K7) and (K8) on the embeddings σ_i^ϵ (in place of σ_i) are replaced by the following parametrized radius inequality. The embeddings σ_i^ϵ satisfy conditions (K1) to (K6) and are also required to satisfy two further conditions:

(K7ϵ) For $i = 1, 2$, the disk L_i contains a point $(2, \theta_i)$ such that the image under σ_i^ϵ of the vertical segment $(2, \theta_i) \times [-2, 2] \subset D_i \subset \mathbb{W}$ is contained in $\{r = 2 + \epsilon\} \cap \{\theta_i^- \leq \theta \leq \theta_i^+\}$, and for $\epsilon = 0$ it is contained in the periodic orbit $\mathcal{O}_i$.

(K8ϵ) *Parametrized Radius Inequality*: For all $x' = (r', \theta', -2) \in L_i^-$, let $(r, \theta, z) = \sigma_i^\epsilon(r', \theta', -2) \in \mathcal{L}_i^{\epsilon-}$, then $r < r' + \epsilon$ unless $x' = (2, \theta_i, -2)$ and then $r = 2 + \epsilon$.

Observe that for $\epsilon = 0$, we recover the Radius Inequality of Kuperberg, one of the most fundamental concepts of Kuperberg's construction. Figure 1.28 represents the radius inequality for $\epsilon < 0$, $\epsilon = 0$, and $\epsilon > 0$. Note that in the third illustration (c) the insertion has a vertical shift upwards. This is not required by conditions (K7ϵ) and (K8ϵ), but it is used to prove the third part of Theorem 1.5.1.

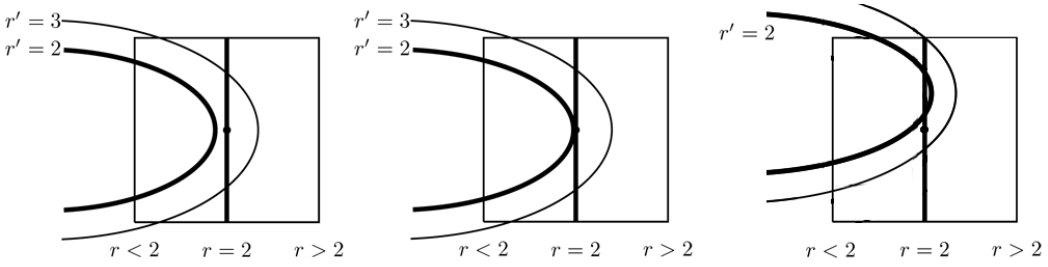

(a) $\epsilon < 0$ (b) $\epsilon = 0$ (c) $\epsilon > 0$

Figure 1.28: The modified radius inequality for the cases $\epsilon < 0$, $\epsilon = 0$ and $\epsilon > 0$

The case $\epsilon < 0$

In the case $\epsilon < 0$, the self-insertions do not penetrate far enough as to trap the periodic orbits. Condition (K8ϵ) implies that the radius always grows at secondary entry points (without any exceptions). For these plugs Proposition 1.3.1 is still valid. As a corollary we obtain that the $\mathcal{K}_\epsilon$-orbits containing the arcs $\mathcal{O}_i^\epsilon = \mathcal{O}_i \cap \mathbb{W}'_\epsilon$ of the Wilson periodic orbits are periodic. Here

$$\mathbb{W}'_\epsilon = \mathbb{W} - (\sigma_1^\epsilon(D_1) \cup \sigma_2^\epsilon(D_2)),$$

in analogy with the definition of $\mathbb{W}'$ (1.5). As stated in Theorem 1.5.1, these two orbits are the only two periodic orbits of the flow in $\mathbb{K}_\epsilon$. The proof of this last assertion is basically the same as the proof of the aperiodicity of $\mathbb{K} = \mathbb{K}_0$.

What I want to point out about this case is that it gives another way of understanding the minimal set of the original Kuperberg plug $\mathbb{K} = \mathbb{K}_0$. In fact, the two periodic orbits of $\mathbb{K}_\epsilon$ for $\epsilon < 0$ bound an invariant cylinder C_ϵ that is obtained by flowing inside $\mathbb{K}_\epsilon$ the notched Reeb cylinder $\mathcal{R}'_\epsilon = \mathcal{R} \cap \mathbb{W}'_\epsilon$. Indeed, repeating the analysis in Section 1.3.2 we first point out that Proposition 1.3.4 is valid and we can consider as level 0 the set $\tau_\epsilon(\mathcal{R}'_\epsilon)$ (where τ_ϵ is defined as τ). This set intersects each entrance of an insertion along a curve contained in the region $\{r > 2\}$ and thus each curve generates a finite propeller that is at level 1 (see Figure 1.18 for an illustration of a finite propeller in $\mathbb{W}$).

As ϵ increases to zero, the length of these two level 1 propellers grows and when $\epsilon = 0$ the propellers become infinite. Hence for ϵ small enough, these two propellers at level 1 intersect the insertions and thus give birth to propellers at level 2, etc. So we can build the cylinder C_ϵ as we built $\mathfrak{M}_0$ in Section 1.3.2. The main difference is that for C_ϵ the process stops: the level 1 propellers are finite and thus intersect the insertions a finite number of times and this repeats at any level, and the maximum level attained in C_ϵ is upper bounded by a number that depends only on ϵ. The set C_ϵ is thus the union of the notched Reeb cylinder $\tau_\epsilon(\mathcal{R}'_\epsilon)$ and a finite number of finite propellers.

A flattened illustration of C_ϵ is basically the same as Figure 1.24, except that the two vertical level one propellers $\tau(P'_\gamma)$ and $\tau(P'_\lambda)$ are finite propellers, implying that the process described by Figures 1.22 and 1.24 stops. The length of the two level 1 propellers increases as ϵ increases to zero, thus the complexity of the flattened diagram increases. We thus obtain an approximation of $\mathfrak{M}_0$ by embedded cylinders in $\mathbb{R}^3$.

The case $\epsilon > 0$

The Radius Inequality in this case is illustrated in Figure 1.28 (c). Along the vertical line $\{r = 2\}$ the r'-coordinate is bounded below by $2 - \epsilon$, while the vertical line $\{r = 3\}$ does not intersects the insertion. This implies that there are values (between $2 + \epsilon$ and 3), let me call one of them a, of the radius such that along the vertical line $\{r = a\}$ the r'-coordinate is bounded below by a. In [P7] we assume (for simplicity) that there is a unique such value, denoted by r_ϵ (see Lemma 1.6.5 and Hypothesis 1.6.6 in the following section for a precise statement). Thus for points with $r > r_\epsilon$, we have that the radius coordinate grows at secondary entry points. This implies that Proposition 1.3.1 is valid when the hypothesis $r > 2$ is replaced by $r > r_\epsilon$.

We can thus repeat the construction of the maps ϕ_1^+, ϕ_2^+, ϕ_1^- and ϕ_2^- in Section 1.4 and understand their action on points with radius coordinate bigger than r_ϵ in the rectangle $\mathbf{R}_0$ (for $\mathbf{R}_0$ as in Section 1.4).

In order to prove Theorem 1.5.1 for $\epsilon > 0$ we consider words in the generators $\{Id, \phi_1^+, \widehat{\Psi}\}$ and their inverses, for $\widehat{\Psi}$ as in (1.11). The proof then follows in two steps:

1. find a set $V_0 \subset \mathbf{R}_0$ for which there exists $\ell(\epsilon) \in \mathbb{N}$ such that for every $k \geq \ell(\epsilon)$ and $\varphi_k = \widehat{\Psi}^k \circ \phi_1^+$ we have that
   — $U_k = \varphi_k(V_0) \cap V_0 \neq \emptyset$;
   — $\varphi_k(U_k) \cap U_k$ has two connected components.
2. proving that the invariant set of the maps φ_k, for each $k \geq \ell(\epsilon)$, is an invariant set of the flow and that the return times to these sets are bounded.

The first point guarantees the existence of a countable number of horseshoe like dynamics in the pseudo⋆group generated by $\{Id, \phi_1^+, \widehat{\Psi}\}$. The second one says that these horseshoes are embedded in the flow and the fact that the return times are bounded, allows to conclude that the topological entropy of the flow is positive. The vertical shift in Figure 1.28 is used to prove this second point.

We do not understand how these horseshoes change as $\epsilon \to 0$ and disappear in the plug $\mathbb{K}_0$. One thing I understand is that the return times to the invariant sets grow as ϵ decreases, but the

aspect that is not clear is what happens with all the periodic orbits in the plugs $\mathbb{K}_\epsilon$ for $\epsilon > 0$. Is it just that their lengths blow up?

The bifurcation that is made explicit in Theorem 1.5.1 is highly not generic, but it might be surrounded by some type of generic bifurcations in the space of non-singular vector fields. Can we say something about nearby bifurcations?

1.6 Generic hypotheses

The construction of aperiodic Kuperberg flows involve multiple choices, which do not change whether the resulting flows are aperiodic, but do impact other dynamical properties of these flows. In this section, I present the assumptions made in the works [P5, P7], that are grouped under the word *generic* in the previous sections. In [P10] we discuss properties of the flow that depend on the generic hypotheses and discuss possible situations that can arise if these assumptions are dropped. This section thus gives a quick list of the hypotheses that were briefly explained in Remark 1.2.1. We discuss first the case for the traditional Kuperberg flows and afterward discuss the variations of the construction to obtain the family $\mathbb{K}_\epsilon$ described in Section 1.5.

Recall that the modified Wilson vector field on $\mathbb{W}$ is given in (1.2) by

$$\mathcal{W} = g(r,\theta,z)\frac{\partial}{\partial z} + f(r,\theta,z)\frac{\partial}{\partial \theta}$$

where the function $g(r,\theta,z) = g(r,z)$ is the function $g\colon \mathbf{R} \to [0, g_0]$ which is non-negative, vanishing only at the points $(2,\pm 1)$ and symmetric about the line $\{z = 0\}$. The function $f(r,\theta,z) = f(r,z)$ is assumed to satisfy the conditions (W1) to (W5).

Figure 1.3 illustrates the dynamics of the flow of $\mathcal{W}$ restricted to the cylinders $\{r = cst.\}$ in $\mathbb{W}$, for various values of the radius. It is clear from these pictures that the interesting part of the dynamics of this flow occurs on the cylinders with radius near to 2 and near the periodic orbits $\mathcal{O}_i$ for $i = 1, 2$.

The points $(2,\pm 1) \in \mathbf{R}$ are the local minimum or maximum for the function g and thus its matrix of first derivatives must also vanish at these points and the Hessian matrix of second derivatives must be positive semi-definite. The generic property for such a function is that the Hessian matrix for g at these points is positive definite. In the works [P5, P7], a more precise version of this was formulated:

HYPOTHESIS 1.6.1. *The function g satisfies the following conditions:*

$$g(r,z) = g_0 \quad \textit{for} \quad (r-2)^2 + (|z|-1)^2 \geq \epsilon_0^2 \tag{1.17}$$

where $0 < \epsilon_0 < 1/4$ is sufficiently small. Moreover, we require that the Hessian matrices of second partial derivatives for g at the vanishing points $(2,\pm 1)$ are positive definite. In addition, we require that $g(r,z)$ is monotone increasing as a function of the distance $\sqrt{(r-2)^2 + (|z|-1)^2}$ from the points $(2,\pm 1)$.

Many of the results in [P5, P7] require this generic hypotheses for their proofs, as it allows making estimates on the speed of ascent for the orbits of the Wilson flow near the periodic orbits.

The choices for the embeddings $\sigma_i\colon D_i \to \mathbb{W}$, for $i = 1, 2$, as illustrated on Figures 1.7 and 1.8, are more wide-ranging and have a fundamental influence on the dynamics of the resulting Kuperberg flows on the quotient space $\mathbb{K}$. We first impose a "normal form" condition on the insertions, which

does not have significant impact on the dynamics, but allows a more straightforward formulation of the other properties of the insertion maps.

Let $(r, \theta, z) = \sigma_i(x') \in \mathcal{D}_i$ for $i = 1, 2$, where $x' = (r', \theta', z') \in D_i$ is a point in the domain of σ_i. Let $\pi_z(r, \theta, z) = (r, \theta, -2)$ denote the projection of $\mathbb{W}$ along the z-coordinate. We assume that σ_i restricted to the bottom face, $\sigma_i \colon L_i^- \to \mathbb{W}$, has image transverse to the vertical fibers of π_z. This normal form can be achieved by an isotopy of a given embedding along the flow lines of the vector field $\mathcal{W}$, so does not change the orbit structure of the resulting vector field on the plug $\mathbb{K}$.

The above transversality assumption implies that $\pi_z \circ \sigma_i \colon L_i^- \to \mathbb{W}$ is a diffeomorphism into the face $\partial_h^- \mathbb{W}$, with image denoted by $\mathfrak{D}_i \subset \partial_h^- \mathbb{W}$. Then let $\vartheta_i = (\pi_z \circ \sigma_i)^{-1} \colon \mathfrak{D}_i \to L_i^-$ denote the inverse map, so we have:

$$\vartheta_i(r, \theta, -2) = (r(\vartheta_i(r, \theta, -2)), \theta(\vartheta_i(r, \theta, -2)), -2) = (R_{i,r}(\theta), \Theta_{i,r}(\theta), -2) \ . \tag{1.18}$$

We can then formalize in terms of the maps ϑ_i the assumptions on the insertion maps σ_i.

HYPOTHESIS 1.6.2 (*Strong Radius Inequality*)**.** *For $i = 1, 2$, assume that:*

1. *$\sigma_i \colon L_i^- \to \mathbb{W}$ is transverse to the fibers of π_z;*
2. *$r = r(\sigma_i(r', \theta', z')) < r'$, except for $(2, \theta_i, z')$ and then $z(\sigma_i(2, \theta_i, z')) = (-1)^i$;*
3. *$\Theta_{i,r}(\theta) = \theta(\vartheta_i(r, \theta, -2))$ is an increasing function of θ for each fixed r;*
4. *$R_{i,r}(\theta) = r(\vartheta_i(r, \theta, -2))$ has non-vanishing derivative for $r = 2$, except for the case of $\overline{\theta_i}$ defined by $\vartheta_i(2, \overline{\theta_i}, -2) = (2, \theta_i, -2)$;*
5. *For r sufficiently close to 2, we require that the θ derivative of $R_{i,r}(\theta)$ vanish at a unique point denoted by $\overline{\theta}(i, r)$, with $\overline{\theta}(i, 2) = \overline{\theta}_i$.*

Consequently, each surface $\mathcal{L}_i^-$ is transverse to the coordinate vector fields $\partial/\partial\theta$ and $\partial/\partial z$ on $\mathbb{W}$.

The illustration of the image of the curves $\{r' = 2\}$ and $\{r' = 3\}$ on Figure 1.8 suggests that these curves have "parabolic shape". We formulate this notion more precisely using the function $\vartheta_i(r, \theta, -2)$ defined by (1.18) and introduce the more general hypotheses they may satisfy. Recall that $\epsilon_0 > 0$ was introduced in Hypothesis 1.6.1.

HYPOTHESIS 1.6.3. *For $i = 1, 2$, $2 \leq r_0 \leq 2 + \epsilon_0$ and $\theta_i - \epsilon_0 \leq \theta \leq \theta_i + \epsilon_0$, assume that*

$$\frac{d}{d\theta}\Theta_{i,r_0}(\theta) > 0 \quad , \quad \frac{d^2}{d\theta^2}R_{i,r_0}(\theta) > 0 \quad , \quad \frac{d}{d\theta}R_{i,r_0}(\overline{\theta_i}) = 0 \ . \tag{1.19}$$

where $\overline{\theta_i}$ satisfies $\vartheta_i(2, \overline{\theta_i}, -2) = (2, \theta_i, -2)$. Thus for $2 \leq r_0 \leq 2 + \epsilon_0$, the graph of $R_{i,r_0}(\theta)$ is convex upwards with vertex at $\theta = \overline{\theta_i}$.

Hypothesis 1.6.3 implies that all of the level curves $\{r' = c\}$, for $2 \leq c \leq 2 + \epsilon_0$, have parabolic shape, as the illustration in Figure 1.8 suggests.

We can now define what is called a generic Kuperberg flow in the work [P5].

DEFINITION 1.6.4. *A Kuperberg flow Φ_t is* generic *if the Wilson flow $\mathcal{W}$ used in the construction of the vector field $\mathcal{K}$ satisfies Hypothesis 1.6.1 and the insertion maps σ_i for $i = 1, 2$ used in the construction of $\mathbb{K}$ satisfies Hypotheses 1.6.2, and Hypotheses 1.6.3.*

That is, the singularities for the vanishing of the vertical component $g \cdot \partial/\partial z$ of the vector field $\mathcal{W}$ are of quadratic type and the insertion maps used to construct $\mathbb{K}$ yield quadratic radius functions near the special points.

Recall that the insertion maps for the variations from a Kuperberg flow as introduced in Section 1.5 are denoted by $\sigma_i^\epsilon \colon D_i \to \mathbb{W}$, for $i = 1, 2$. It is assumed that these maps satisfy the

modified conditions (K7ϵ) and (K8ϵ). The illustrations of the radius inequality in Figure 1.28 again suggest that the images of the curves $\{r' = c\}$ are of "quadratic type". For $\epsilon < 0$ there is no need to make any further assumptions in the construction in order to obtain Theorem 1.5.1. In contrast, for $\epsilon > 0$ we need the analog of the generic hypotheses in Definition 1.6.4 and the existence of the radius r_ϵ as discussed in Section 1.5 and below.

We again assume the insertion maps $\sigma_i^\epsilon \colon L_i^- \to \mathbb{W}$ are transverse to the fibers of the projection map $\pi_z \colon \mathbb{W} \to \partial_h^- \mathbb{W}$ along the z-coordinate. Then we can define the inverse map

$$\vartheta_i^\epsilon = (\pi_z \circ \sigma_i^\epsilon)^{-1} \colon \mathfrak{D}_i \to L_i^-$$

and express the inverse map in polar coordinates as:

$$\vartheta_i^\epsilon(r, \theta, -2) = (r(\vartheta_i^\epsilon(r, \theta, -2)), \theta(\vartheta_i^\epsilon(r, \theta, -2)), -2) = (R_{i,r}^\epsilon(\theta), \Theta_{i,r}^\epsilon(\theta), -2) \ . \tag{1.20}$$

Then the level curves $r' = c$ pictured in Figure 1.28 are given by the maps $\theta' \mapsto \pi_z(\sigma_i^\epsilon(c, \theta', -2)) \in \partial_h^- \mathbb{W}$.

We note a straightforward consequence of the Parametrized Radius Inequality (K8ϵ). Recall that θ_i is the radian coordinate specified in (K8ϵ) such that for $x' = (2, \theta_i, -2) \in L_i^-$ we have $r(\sigma_i^\epsilon(2, \theta_i, -2)) = 2 + \epsilon$. I refer to Lemma 6.1 in [P7].

LEMMA 1.6.5. *For $\epsilon > 0$ there exists $2 + \epsilon < r_\epsilon < 3$ such that $r(\sigma_i^\epsilon(r_\epsilon, \theta_i, -2)) = r_\epsilon$.*

We then add an additional assumption on the insertion maps σ_i^ϵ for $i = 1, 2$ which specifies the qualitative behavior of the radius function for $r \geq r_\epsilon$.

HYPOTHESIS 1.6.6. *If r_ϵ is the smallest $2+\epsilon < r_\epsilon < 3$ such that $r(\sigma_i^\epsilon(r_\epsilon, \theta_i, -2)) = r_\epsilon$. Assume that $r(\sigma_i^\epsilon(r, \theta_i, -2)) < r$ for $r > r_\epsilon$.*

The conclusion of Hypothesis 1.6.6 is implied by the Radius Inequality for the case $\epsilon = 0$, but does not follow from the condition (K8ϵ) when $\epsilon > 0$.

We can now formulate the analog of Hypothesis 1.6.2, which imposes uniform conditions on the derivatives of the maps ϑ_i^ϵ, for the plugs $\mathbb{K}_\epsilon$ with $\epsilon > 0$. Recall that $0 < \epsilon_0 < 1/4$ was specified in Hypothesis 1.6.1 and we assume that $0 < \epsilon < \epsilon_0$.

HYPOTHESIS 1.6.7 (*Strong Radius Inequality*)**.** *For $i = 1, 2$, assume that:*

1. *$\sigma_i^\epsilon \colon L_i^- \to \mathbb{W}$ is transverse to the fibers of π_z;*
2. *$r = r(\sigma_i^\epsilon(r', \theta', z)) < r + \epsilon$, except for $x' = (2, \theta_i, z)$ and then $r = 2 + \epsilon$;*
3. *$\Theta_{i,r}^\epsilon(\theta)$ is an increasing function of θ for each fixed r;*
4. *For $2 - \epsilon_0 \leq r \leq 2 + \epsilon_0$ and $i = 1, 2$, assume that $R_{i,r}^\epsilon(\theta)$ has non-vanishing derivative, except when $\theta = \overline{\theta_i}$ as defined by $\vartheta_i^\epsilon(2 + \epsilon, \overline{\theta}_i, -2) = (2, \theta_i, -2)$;*
5. *For r sufficiently close to $2 + \epsilon$, we require that the θ derivative of $R_{i,r}^\epsilon(\theta)$ vanishes at a unique point denoted by $\overline{\theta}(i, r)$.*

Note that Hypotheses 1.6.6 and 1.6.7 combined imply that r_ϵ is the unique value of $2+\epsilon < r_\epsilon < 3$ for which $r(\sigma_i^\epsilon(r_\epsilon, \theta_i, -2)) = r_\epsilon$. We can then formulate the analog of Hypothesis 1.6.3.

HYPOTHESIS 1.6.8. *For $2 - \epsilon_0 \leq r_0 \leq 2 + \epsilon_0$ and $\theta_i - \epsilon_0 \leq \theta \leq \theta_i + \epsilon_0$, assume that*

$$\frac{d}{d\theta}\Theta_{i,r_0}^\epsilon(\theta) > 0 \quad , \quad \frac{d^2}{d\theta^2}R_{i,r_0}^\epsilon(\theta) > 0 \quad , \quad \frac{d}{d\theta}R_{i,r_0}^\epsilon(\overline{\theta_i}) = 0 \ . \tag{1.21}$$

where $\overline{\theta_i}$ satisfies $\vartheta_i^\epsilon(2, \overline{\theta_i}, -2) = (2, \theta_i, -2)$. Thus for $2 - \epsilon_0 \leq r_0 \leq 2 + \epsilon_0$, the graph of $R_{i,r_0}^\epsilon(\theta)$ is convex upwards with vertex at $\theta = \overline{\theta_i}$.

Finally, we have the definition of the generic Φ_t^ϵ flows of the plugs $\mathbb{K}_\epsilon$, as introduced in Section 1.5 and studied in [P7].

DEFINITION 1.6.9. *The flow Φ_t^ϵ is* generic *if the Wilson flow $\mathcal{W}$ used in the construction of the vector field $\mathcal{K}_\epsilon$ satisfies Hypothesis 1.6.1 and the insertion maps σ_i^ϵ for $i = 1, 2$ used in the construction of $\mathbb{K}_\epsilon$ satisfies Hypotheses 1.6.7, and Hypotheses 1.6.8.*

Chapter 2

Trunkenness, an asymptotic invariant for flows

This chapter covers the results of my work with P. Dehornoy [P9]. The problem we address is the construction of new invariants of volume-preserving vector fields on $\mathbb{S}^3$, or on compact domains of $\mathbb{R}^3$, up to volume-preserving diffeomorphisms. This problem is motivated by at least two physical situations. First if v is the velocity field of a time-dependent ideal fluid satisfying the Euler equations (ideal hydrodynamics) then its vorticity field $\operatorname{curl} v$ is transported by the flow of v [Hel1858]. Second if B is the magnetic field of an incompressible plasma (ideal magnetodynamics), then B turns out to be transported by the velocity field as long as the latter does not develop singularities [Wol58]. In these contexts, invariants of $\operatorname{curl} v$ or B up to volume-preserving diffeomorphisms yield time-independent invariants of the system.

Not so many such invariants exist. The first one was discovered by W. Thomson [Tho1867]: if the considered field has a periodic orbit or a periodic tube, then its knot type is an invariant (this remark led to the development of knot theory by P. G. Tait [Tait1877]). However it may not be easy to find periodic orbits and even then such an invariant only takes a small part of the field into account.

The main known invariant is called *helicity*. It is defined by the formula $\mathrm{Hel}(v) = \int v \cdot u$, where $u = \operatorname{curl}^{-1}(v)$ is an arbitrary vector-potential of v. It was discovered by Woltjer, Moreau and Moffatt [Wol58, Mor61, Mof69]. Helicity is easy to compute or to approximate since it is enough to exhibit a vector-potential of the considered vector field, to take the scalar product and to integrate. The connection with knot theory was sketched by Moffatt [Mof69] and deepened by Arnold [Arn73] as follows. Denote by $k_X(p,t)$ a loop starting at the point p, tangent to the vector field X for a time t and closed by an arbitrary segment of bounded length. Denote by Lk the linking number of loops. Arnold showed that for almost every p_1, p_2, the limit $\lim\limits_{t_1,t_2\to\infty} \dfrac{1}{t_1 t_2}\mathrm{Lk}(k_X(p_1,t_1), k_X(p_2,t_2))$ exists (see also [Vog02] for a corrected proof). Moreover, if X is ergodic the limit coincides almost everywhere with $\mathrm{Hel}(X)$ (for a non-ergodic vector field, one has to average the previous limit to obtain the helicity).

The idea of considering knot invariants of long pieces of orbits of the vector field was pursued by Gambaudo and Ghys [GG01] who considered ω-signatures of knots, Baader [Baa11] who considered linear saddle invariants, and Baader and Marché [BM12] who considered Vassiliev's finite type invariants. In every case, it is shown that $\lim_{t\to\infty} \frac{1}{t^n} V(k_X(p,t))$ exists, where V is the considered invariant and n a suitable exponent called the *order* of the asymptotic invariant. However all these constructions have the drawback that they do not yield any new invariant for ergodic vector fields, since the obtained limits are all functions of the helicity.

Recently, it was proved by Kudryavtseva for vector fields obtained by suspending an area-preserving diffeomorphism of a surface [Kud14] and for non-vanishing vector fields [Kud16] and then by Enciso, Peralta-Salas and Torres de Lizaur [EPT16] for arbitrary volume-preserving vector fields, that every invariant that is *regular integral* (in the sense that its Fréchet derivative is the integral of a continuous kernel) is a function of helicity. I will not state the precise statements. These results give a satisfactory explanation of why most constructions yield invariants that are functions of helicity for ergodic vector fields. However they do not rule out the existence of other invariants, but imply that such invariants cannot be *too* regular.

An example of such another invariant is the asymptotic crossing number considered by Freedman and He [FH91]. The advantage is that it is not proportional to helicity, but the disadvantage is that it is hard to compute, even on simple examples.

In [P9] we consider a less well-known knot invariant called the trunk (see Definition 2.0.1 below). It was defined by Ozawa [Ozw10], building on the concept of *thin position* that was introduced by Gabai [Gab87] for solving the R-conjecture. Less famous than the invariants previously studied in the context of vector fields, the trunk has the advantage that its definition relies on surfaces transverse to the considered knot, so that it is easy to transcript in the context of vector fields. The invariant depends on an invariant measure for the flow of the vector field that may or may not be a volume and is invariant under homeomorphisms that preserve this measure. Given a μ-preserving vector field X and a surface S, the *geometric flux* through S is the infinitesimal volume that crosses S in both directions (see Definition 2.0.4), we denote it by $\mathrm{Flux}(X, \mu, S)$. Our invariant is a minimax of the geometric flux, where one minimizes over all height functions and maximizes over the levels of the considered height function.

To motivate our definition, I will start by defining the trunk of a knot. Let K be a knot, embedded in $\mathbb{R}^3$. The *standard height function* on $\mathbb{R}^3$ is the function $h_z : \mathbb{R}^3 \to \mathbb{R}, (x, y, z) \mapsto z$. Every level $h_z^{-1}(t)$ is a 2-dimensional plane. A *height function* on $\mathbb{R}^3$ is a function obtained by precomposing h_z by an orientation preserving diffeomorphism, that is, a function of the form

$$\begin{array}{rcl} h : \mathbb{R}^3 & \to & \mathbb{R} \\ (x, y, z) & \mapsto & h_z(\phi(x, y, z)) \end{array}$$

for ϕ an orientation preserving diffeomorphism of $\mathbb{R}^3$. In particular, a height function is a function whose levels are smooth planes. A height function h is said to be in *Morse position* with respect to K if the restriction of h to K is a Morse function. In this case there are only finitely many points at which K is tangent to a level of h. We denote this set of functions by height Morse functions.

DEFINITION 2.0.1. *Assume that K is an embedded knot in $\mathbb{R}^3$ that is in Morse position with respect to h_z. The* trunk of the curve K relatively to h_z *is*

$$\mathrm{tk}_{h_z}(k) := \max_{t \in \mathbb{R}} \sharp\{K \cap h_z^{-1}(t)\}.$$

The trunk of a knot K *is then defined by*

$$\mathrm{Tk}(K) := \min_{\substack{h \text{ height} \\ \text{Morse function}}} \mathrm{tk}_h(K) = \min_{\substack{h \text{ height} \\ \text{Morse function}}} \max_{t \in \mathbb{R}} \sharp\{K \cap h^{-1}(t)\}.$$

One can define the trunk of a knot by fixing the height function and changing the embedding of the knot in $\mathbb{R}^3$, see [Zup12].

EXAMPLE 2.0.2. *A knot is trivial if and only if its trunk equals* 2*. Indeed the embedding as the boundary of a vertical disk shows that the trunk is less than or equal to* 2 *and every embedding*

in Morse position of the trivial knot has to intersect some horizontal plane in at least two points. Conversely, if the trunk of a knot is equal to 2, then it admits an embedding that intersects every horizontal plane in at most two points. The union of the segments that connect these pairs of points is a disk bounded by the knot, implying that the knot is trivial.

EXAMPLE 2.0.3. *For p, q in $\mathbb{N}$, the torus knot $T(p,q)$ can be realized as the closure of a braid with q strands, yielding $\mathrm{Tk}(T(p,q)) \leq 2q$. By symmetry one also gets $\mathrm{Tk}(T(p,q)) \leq 2p$. Actually, one can prove $\mathrm{Tk}(T(p,q)) = 2\min(p,q)$, see Remark 1.2 in [Ozw10].*

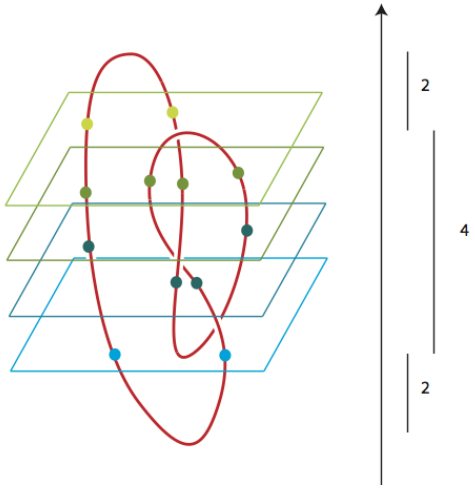

Figure 2.1: The trunk of the trefoil knot

We use Definition 2.0.1 to define the trunkenness of a vector field with respect to an invariant measure. The main question then concerns the analog of the number of intersection points of a surface with a curve when the curve is replaced by a vector field. A natural answer is the *geometric flux*. If X is a vector field that preserves a measure μ given by a volume element Ω, one can then consider the 2-form $\iota_X\Omega$. For S a piece of oriented surface that is positively transverse to X, the integral $\int_S \iota_X\Omega$ computes the instantaneous volume that crosses S. In other words, by Fubini Theorem we have $\mu(\phi^{[0,t]}(S)) = (\int_S \iota_X\Omega)\cdot t$. On the other hand if S is negatively transverse to X we have $\mu(\phi^{[0,t]}(S)) = -(\int_S \iota_X\Omega)\cdot t$. Therefore in this case, for any surface S, the instantaneous volume crossing S is given by $\int_S |\iota_X\Omega|$. Now if the measure μ is not given by integrating a volume form one cannot consider the above integral, but the quantity $\mu(\phi^{[0,t]}(S))$ still makes sense for any piece of surface S.

DEFINITION 2.0.4. *For X a vector field that preserves a measure μ and a surface S, the* geometric flux *of (X,μ) through S is*

$$\mathrm{Flux}(X,\mu,S) := \lim_{\epsilon\to 0} \frac{1}{\epsilon}\,\mu(\phi^{[0,\epsilon]}(S)).$$

This definition generalizes the number of intersection points of a knot with a surface. Indeed one can see an embedding k of a knot K as a vector field with a particular invariant measure in the following way: on K, consider a non-singular vector field X_k that is tangent to k at every point and denote by ϕ_k^t the induced flow. Since k is closed, ϕ_k is T_k-periodic for some $T_k > 0$. The Dirac linear measure associated to X_k is defined by

$$\mu_k(A) = \mathrm{Leb}(\{t \in [0,T_k], \phi_k^t(x) \in A\})$$

where A is a measurable set and x an arbitrary point on k. The measure μ_k is X_k-invariant and has total mass T_k. In this setting, for S a surface that intersects k in finitely many points, a point p in the set $k\cap S$ has μ_k-measure zero and thus cannot be detected by the measure. But by definition of μ_k the set $\phi_k^{[0,\epsilon]}(p)$ is an arc of k of μ_k-measure ϵ and since $k\cap S$ is made of finitely many points, for ϵ small enough, the set $\phi_k^{[0,\epsilon]}(k\cap S)$ has μ_k-measure exactly $\epsilon\cdot\sharp\{k\cap S\}$. In other words, one has

$$\sharp\{k\cap S\} = \lim_{\epsilon\to 0}\frac{1}{\epsilon}\,\mu_k(\phi_k^{[0,\epsilon]}(k\cap S)).$$

As μ_k is concentrated on k, we thus have

$$\sharp\{k \cap S\} = \lim_{\epsilon \to 0} \frac{1}{\epsilon} \mu_k(\phi_k^{[0,\epsilon]}(S)) = \mathrm{Flux}(X_k, \mu_k, S), \tag{2.1}$$

so the geometric flux indeed generalizes the number of intersection points.

We now mimic for vector fields the definition of the trunk of a knot. In order to have a well-defined maximum, in what follows we assume the vector fields are on a compact domain $D^3 \subset \mathbb{R}^3$ or on the 3-sphere $\mathbb{S}^3 = \mathbb{R}^3 \cup \infty$. In the later case, we define the *standard height function*

$$\begin{array}{rcl} h_0 : \mathbb{S}^3 & \to & [0,1] \\ (x,y,z) & \mapsto & 1 - \dfrac{1}{1+x^2+y^2+z^2}. \end{array}$$

The levels $h_0^{-1}(0)$ and $h_0^{-1}(1)$ consist of the points $(0,0,0)$ and ∞ respectively and every other level $h_0^{-1}(t)$ is a 2-dimensional sphere centered at the origin. A *height function* on $\mathbb{S}^3$ is then a function obtained by precomposing by an orientation preserving diffeomorphism ϕ of $\mathbb{S}^3$, that is, a function of the form $h : \mathbb{S}^3 \to [0,1], (x,y,z) \mapsto h_0(\phi(x,y,z))$.

DEFINITION 2.0.5. *Let X be a vector field whose flow preserves a measure μ on a compact domain of $\mathbb{R}^3$ or on $\mathbb{S}^3$ and h a height function. We set*

$$\mathrm{tks}_h(X,\mu) := \max_{t\in[0,1]} \mathrm{Flux}(X,\mu,h^{-1}(t)) = \max_{t\in[0,1]} \lim_{\epsilon\to 0} \frac{1}{\epsilon}\mu(\phi^{[0,\epsilon]}(h^{-1}(t))).$$

The trunkenness of (X,μ) *is defined as*

$$\begin{array}{rcl} \mathrm{Tks}(X,\mu) := \inf\limits_{\substack{h \text{ height} \\ \text{function}}} \mathrm{tks}_h(X,\mu) & = & \inf\limits_{\substack{h \text{ height} \\ \text{function}}} \max\limits_{t\in[0,1]} \mathrm{Flux}(X,\mu,h^{-1}(t)) \\ & = & \inf\limits_{\substack{h \text{ height} \\ \text{function}}} \max\limits_{t\in[0,1]} \lim\limits_{\epsilon\to 0} \dfrac{1}{\epsilon}\mu(\phi^{[0,\epsilon]}(h^{-1}(t))). \end{array}$$

Note that we can only consider an infimum instead of a minimum as in the case of knots. In Theorem 2.0.11 we study the implications of having a height function achieving the trunkenness.

If the invariant measure μ is given by the integration of a volume form Ω, we get the alternative definitions

$$\mathrm{tks}_h(X,\Omega) = \max_{t\in[0,1]} \int_{h^{-1}(t)} |\iota_X\Omega|, \quad \text{and} \quad \mathrm{Tks}(X,\Omega) = \inf_{\substack{h \text{ height} \\ \text{function}}} \max_{t\in[0,1]} \int_{h^{-1}(t)} |\iota_X\Omega|.$$

From Definition 2.0.5 it is straightforward that the trunkenness of a vector field is invariant under diffeomorphisms that preserve the measure μ. More is true, the trunkenness is invariant under homeomorphisms that preserve μ.

THEOREM 2.0.6. *Assume that X_1 and X_2 are vector fields on $\mathbb{S}^3$ or on a compact domain of $\mathbb{R}^3$ that preserve a probability measure μ and that there is a μ-preserving homeomorphism f that conjugates the flows of X_1 and X_2. Then we have*

$$\mathrm{Tks}(X_1,\mu) = \mathrm{Tks}(X_2,\mu).$$

What we do in [P9] is to prove several properties of this new invariant. The first one is a continuity result, that is more easily stated in terms of currents, but we also provide corollaries that do not rely on this vocabulary. Given a vector field X and a measure μ, we can define a normal 1-current $C_{(X,\mu)}$: for α any differential 1-form $C_{(X,\mu)}(\alpha) = \int \alpha(X) d\mu$, where the integral is taken on the ambient space. We consider the space of normal currents endowed with the mass topology (see [Mor00]).

THEOREM 2.0.7. *The trunkenness is a continuous functional on the space of normal currents.*

COROLLARY 2.0.8. *Suppose that $(X_n, \mu_n)_{n\in\mathbb{N}}$ is a sequence of measure-preserving vector fields such that $(X_n)_{n\in\mathbb{N}}$ converges to X in the C^0-topology and $(\mu_n)_{n\in\mathbb{N}}$ converges to μ in the weak-$*$ sense. Then we have*

$$\lim_{n\to\infty} \mathrm{Tks}(X_n, \mu_n) = \mathrm{Tks}(X, \mu).$$

Now for p a point in the ambient manifold and $t > 0$, denote by $k_X(p, t)$ the closed curve obtained by concatenating the orbit segment between p and $\phi_X^t(p)$ and a short path between these two points. As for the asymptotic linking number, there is a system of short paths such that we obtain a simple closed curve for μ-almost all points and almost all times [Vog02]. The next corollary states that the trunkenness is an asymptotic invariant in the sense of Arnold [AK98] and its order is 1.

COROLLARY 2.0.9. *Assume that X is a μ-preserving vector field and that X is ergodic with respect to μ, then for μ-almost every p the limit*

$$\lim_{t\to\infty} \frac{1}{t}\mathrm{Tk}(k_X(p, t))$$

exists and is equal to $\mathrm{Tks}(X, \mu)$.

Theorem 2.0.7 allows to compute the trunkenness of Seifert flows on $\mathbb{S}^3$, as explained in Section 2.1. These computations in turn show that the trunkenness is not dictated by helicity, even in the case of ergodic vector fields, thus contrasting with most previously known knot-theoretical constructions.

THEOREM 2.0.10. *There is no function f such that for every ergodic volume-preserving vector field X on $\mathbb{S}^3$ one has* $\mathrm{Tks}(X, \mu) = f(\mathrm{Hel}(X, \mu))$.

Finally we address the question of what happens if for a non-singular vector field on $\mathbb{S}^3$ there is a function that achieves the trunkenness, or in other words if the infimum in Definition 2.0.5 is a minimum.

THEOREM 2.0.11. *Let X be a non-singular vector field on $\mathbb{S}^3$ preserving the measure μ and h a height function such that*

$$\mathrm{Tks}(X, \mu) = \max_{t\in[0,1]} \mathrm{Flux}(X, \mu, h^{-1}(t))$$

Then X has an unknotted periodic orbit.

One of the main motivations for constructing topological invariants of a vector field X is to find lower bounds on the energies $\mathrm{E}_p(X) := \int |X|^p \, d\mu$. Indeed since a topological invariant yields a time-independent invariant of the physical system, an energy bound in terms of a topological invariant will also be time-independent, although the energy may vary when the vector field is transported under (volume-preserving) diffeomorphisms. Such energy bounds exist for the helicity and for the asymptotic crossing number. We do not know whether the trunkenness bounds the energy, a possible path towards finding an inequality between the trunk and the energy is to relate the trunk to the crossing number that is itself related to helicity.

2.1 Independence of helicity

As mentioned in the introduction, the helicity is a well-known invariant of vector fields up to volume-preserving diffeomorphism. In this section, all vector fields are on the sphere $\mathbb{S}^3$ and preserve a volume form, that we denote by Ω. For X such a vector field, Cartan's formula implies that $\iota_X\Omega$ is a closed 2-form and since the ambient manifold is simply connected it is exact. We may then write $\iota_X\Omega = d\alpha$, for α some differential 1-form. The helicity of X can be defined as

$$\mathrm{Hel}(X) := \int_{\mathbb{S}^3} \alpha \wedge d\alpha,$$

and does not depends on the choice of the primitive α [AK98].

As we recalled in the introduction, most known asymptotic invariants are in fact proportional to the helicity [Arn73, GG01, Baa11, BM12]. The goal of this section it to prove that the trunkenness of a vector field is not a function of its helicity. In order to do so we compute the trunkenness and the helicity of a vector field that preserves the invariant tori of a Hopf fibration of $\mathbb{S}^3$.

Considering $\mathbb{S}^3$ as the unit sphere $\{(z_1, z_2) \in \mathbb{C}^2, |z_1|^2 + |z_2|^2 = 1\}$, the *Seifert flow of slope* (α, β) is the flow $\phi_{\alpha,\beta}$ given by

$$\phi^t_{\alpha,\beta}(z_1, z_2) := (z_1 e^{i2\pi\alpha t}, z_2 e^{i2\pi\beta t}),$$

generated by the vector field $X_{\alpha,\beta}$. This flow preserves the standard volume form, that is, the volume form Ω_{Haar} associated to the Haar measure of $\mathbb{S}^3$. The flow has two distinctive periodic orbits corresponding to $z_1 = 0$ and $z_2 = 0$ that are trivial knots in $\mathbb{S}^3$. The tori $|z_1/z_2| = r$ for $0 < r < \infty$ are invariant and the flow on each one of them is the linear flow of slope α/β. If α/β is rational, put $\alpha/\beta = p/q$ with $p, q \in \mathbb{N}$ coprime. Then every orbit of $\phi_{\alpha,\beta}$, different from the two trivial ones, is a torus knot of type $T(p, q)$.

The helicity of $\phi_{\alpha,\beta}$ is equal to $\alpha\beta$. To compute it in the rational case $(\alpha, \beta) = (p, q)$ with p, q coprime, observe that all the orbits except two are periodic of period 1. The linking number of an arbitrary pair of such orbits is pq. Therefore the asymptotic linking number (also called asymptotic Hopf invariant) equals pq and, by Arnold's Theorem [Arn73], so does the helicity. For the general case of (α, β) not necessarily rational, it is enough to use the continuity of the helicity, since $X_{\alpha,\beta}$ can be approximated by a sequence of Seifert flows with rational slope.

PROPOSITION 2.1.1. *The trunkenness of the Seifert flow $\phi_{\alpha,\beta}$ with respect to the standard volume form Ω_{Haar} is equal to $2\min(\alpha, \beta)$.*

Proof. Let us first prove $\mathrm{Tks}(X_{\alpha,\beta}, \Omega_{\mathrm{Haar}}) \leq 2\beta$. For this it is enough to exhibit a height function h that yields $\mathrm{tks}_h(X_{\alpha,\beta}, \Omega_{\mathrm{Haar}}) = 2\beta$. First define $\infty = (0, 1)$ and $0 = (0, -1)$ in $\mathbb{S}^3 \subset \mathbb{C}^2$ and take the stereographic projection to identify

$$\{(z_1, z_2) \in \mathbb{C}^2\,,\ |z_1|^2 + |z_2|^2 = 1\} \simeq \mathbb{R}^3 \cup \{\infty\}.$$

Take now as h the standard height function h_0 of $\mathbb{R}^3 \cup \{\infty\}$. The spheres are centered at $0 \in \mathbb{R}^3$ that corresponds to the point $(0, -1) \in \mathbb{S}^3 \subset \mathbb{C}^2$, hence the orbit $z_1 = 0$ intersects twice each level sphere $h_0^{-1}(t)$. The middle sphere, $S = h_0^{-1}(1/2)$, contains the other special orbit $z_2 = 0$ and is the only sphere that intersects all the orbits of $\phi_{\alpha,\beta}$. Then the function $t \mapsto \int_{h_0^{-1}(t)} |\iota_{X_{\alpha,\beta}}\Omega_{\mathrm{Haar}}|$ has a maximum for $t = 1/2$.

For computing $\int_S |\iota_{X_{\alpha,\beta}}\Omega_{\mathrm{Haar}}|$, we remark that the 2-sphere S has the orbit $(e^{i2\pi\alpha t}, 0)$ as an equator, that the flow is positively transverse to the northern hemisphere and negatively transverse to the southern hemisphere. Then the integral $\int_S |\iota_{X_{\alpha,\beta}}\Omega_{\mathrm{Haar}}|$ is equal to twice the flux of $X_{\alpha,\beta}$ through any disk bounded by the curve $(e^{i2\pi\alpha t}, 0)$. Consider the flat disk D in $\mathbb{S}^3$ bounded by $(e^{i2\pi\alpha t}, 0)$. The first return time to D is constant and equal to $1/\beta$, so the flux

multiplied by $1/\beta$ gives the total volume of $\mathbb{S}^3$, that is 1. Therefore $\mathrm{Flux}(X_{\alpha,\beta}, \Omega_{\mathrm{Haar}}, D)$ is equal to β and we obtain $\mathrm{tks}_{h_0}(X_{\alpha,\beta}, \Omega_{\mathrm{Haar}}) = \int_S |\iota_{X_{\alpha,\beta}}\Omega_{\mathrm{Haar}}| = 2\beta$. By symmetry, we then have $\mathrm{Tks}(X_{\alpha,\beta}, \Omega_{\mathrm{Haar}}) \leq 2\min(\alpha, \beta)$.

For proving the converse inequality $\mathrm{Tks}(X_{\alpha,\beta}, \Omega_{\mathrm{Haar}}) \geq 2\min(\alpha, \beta)$, we approximate $X_{\alpha,\beta}$ (in the C^∞-topology) by a sequence $(X_{p_n/r_n, q_n/r_n})_{n\in\mathbb{N}}$, where p_n, q_n, r_n are integer numbers. Theorem 2.0.8 yields

$$\mathrm{Tks}(X_{\alpha,\beta}, \Omega_{\mathrm{Haar}}) = \lim_{n\to\infty} \mathrm{Tks}(X_{p_n/r_n, q_n/r_n}, \Omega_{\mathrm{Haar}}).$$

As the trunkenness is an order-1 invariant (which means that it is multiplied by λ if the vector field is multiplied by λ), we only have to prove $\mathrm{Tks}(X_{p,q}, \Omega_{\mathrm{Haar}}) = 2\min(p, q)$ for p, q two coprime natural numbers.

Since every orbit of $X_{p,q}$ is periodic, we can consider a sequence $(K_n)_{n\in\mathbb{N}}$ of collections of periodic orbits whose induced normalized linear Dirac measures μ_n converge to Ω_{Haar}. We take K_n to be an n-component link all of whose components are torus knots $T(p, q)$. Actually K_n is a cabling with n strands on $T(p, q)$, so by Zupan's theorem [Zup12], the trunk of K_n is $2n\min(p, q)$. Since the period of each component of K_n is 1, the total length of K_n is n and we get

$$\mathrm{Tks}(X_{p,q}, \Omega_{\mathrm{Haar}}) = \lim_{n\to\infty} \mathrm{Tks}(X_{p,q}, \mu_n) = \lim_{n\to\infty} 2\min(p, q) = 2\min(p, q).$$

□

Proof of Theorem 2.0.10. The previous computations show that for a Seifert flow $X_{\alpha,\beta}$ on $\mathbb{S}^3$ we have $\mathrm{Hel}(X_{\alpha,\beta}, \Omega_{\mathrm{Haar}}) = \alpha\beta$ and $\mathrm{Tks}(X_{\alpha,\beta}, \Omega_{\mathrm{Haar}}) = 2\min(\alpha, \beta)$. There is no real function g such that $\min(\alpha, \beta) = g(\alpha\beta)$, so there is no function g such that $\mathrm{Tks}(X_{\alpha,\beta}, \Omega_{\mathrm{Haar}}) = g(\mathrm{Hel}(X_{\alpha,\beta}, \Omega_{\mathrm{Haar}}))$.

However the Seifert flows are not ergodic with respect to Ω_{Haar}. Indeed, the foliation of $\mathbb{S}^3$ by tori is invariant, so that it is easy to construct an invariant set with arbitrary measure. Still, a theorem of Katok [Kat73] states that the vector field $X_{\alpha,\beta}$ can be perturbed (in the C^1-topology) into an ergodic one. Starting from $X_{1,8}$ and $X_{2,4}$ and applying Katok's argument, we obtain two ergodic volume-preserving vector fields $X'_{1,8}$ and $X'_{2,4}$. By continuity, their trunknesses are close to 2 and 4 respectively, while their helicities are close to 8. At the expense of multiplying the $X'_{1,8}$ and $X'_{2,4}$ by a constant, we can assume that their helicities are exactly 8. However their trunknesses are still close to 2 and 4, hence different. □

It is also interesting to compare the formula $\mathrm{Tks}(X_{\alpha,\beta}, \Omega_{\mathrm{Haar}}) = 2\min(\alpha, \beta)$ with Kudryavtseva's and Encisco-Peralata-Salas-Torres de Lizaur's theorems: the function $(\alpha, \beta) \mapsto 2\min(\alpha, \beta)$ is continuous but not differentiable, so that trunkenness is a continuous vector field invariant, but it is not *integral regular* in the sense of [Kud16, EPT16].

Bibliography

[Arn73] V. I. Arnold, *The asymptotic Hopf invariant and its applications*, Proc. Summer School in Diff. Equations at Dilizhan, 1973 (1974), Evevan (in Russian); English transl. Sel. Math. Sov., 5, 327–345, 1986.

[AK98] V. I. Arnold and B. Khesin, Topological methods in hydrodynamics, Appl. Math. Sci., 125, Springer, 1998.

[Baa11] S. Baader, *Asymptotic concordance invariants for ergodic vector fields*, Comment. Math. Helv., 86, 1–12, 2011.

[BM12] S. Baader and J. Marché, *Asymptotic Vassiliev invariants for vector fields*, Bull. Soc. Math. France, 140, 569–582, 2012.

[BS90] M. Barge and R. Swanson, *Pseudo-orbits and topological entropy*, Proc. of the A.M.S, 109, 2, 559–566, 1990.

[Bor68] K. Borsuk, *Concerning homotopy properties of compacta*, Fund. Math., 62, 223–254, 1968.

[Bor69] K. Borsuk, *On movable compacta*, Fund. Math., 66, 137–146, 1969.

[Bor75] K. Borsuk, Theory of shape, Monografie Mat., vol. 59, Polish Science Publ., Warszawa, 1975.

[Bow71] R. Bowen, *Entropy for group endomorphisms and homogeneous spaces*, Trans. Amer. Math. Soc., 153, 401–414, 1971.

[P9] P. Dehornoy and A. Rechtman, *The trunkenness of a volume-preserving vector field*, to appear in Nonlinearity.

[EPT16] A. Enciso, D. Peralta-Salas and F. Torres de Lizaur, *Helicity is the only integral invariant of volume-preserving transformations*, Proc. Natl. Acad. Sci. USA, 113, 2035–2040, 2016.

[FH91] M. H. Freedman and Z.-X. He, *Divergence-Free Fields: Energy and Asymptotic Crossing Number*, Ann. of Math., 134, 189–229, 1991.

[Gab87] D. Gabai, *Foliations and the topology of 3-manifolds III*, J. Differential Geom., 26, 479–536, 1987.

[GG01] J.-M. Gambaudo and É. Ghys, *Signature asymptotique d'un champ de vecteurs en dimension 3*, Duke Math. J., 106, 41–79, 2001.

[Ghys95] É. Ghys, *Construction de champs de vecteurs sans orbite périodique (d'après Krystyna Kuperberg)*, Séminaire Bourbaki, Vol. 1993/94, Exp. No. 785, Astérisque, 227, 283–307, 1995.

[GLW88] É. Ghys, R. Langevin and P. Walczak, *Entropie géométrique des feuilletages*, Acta Math., 160, 105–142, 1988.

[Han80] M. Handel, *One-dimensional minimal sets and the Seifert conjecture*, Ann. of Math. (2), 111, 35–66, 1980.

[Har88] J.C. Harrison, *C^2 counterexamples to the Seifert conjecture*, Topology, 27, 249–278, 1988.

[Hel1858] H. von Helmholtz, *Über Integrale der hydrodynamischen Gleichungen, welche den Wirbelbewegungen entsprechen*, J. Reine Angew. Math., 55, 25–55, 1858.

[Hof93] H. Hofer, *Pseudoholomorphic curves in symplectizations with applications to the Weinstein conjecture in dimension three*, Invent. Math., 114, 3, 515–563, 1993.

[HI] S. Hurder and D. Ingebretson, *Smooth flows with fractional entropy dimension*, in preparation.

[P5] S. Hurder and A. Rechtman, *The dynamics of generic Kuperberg flows*, Astérisque, 377, 1–250, 2016.

[P7] S. Hurder and A. Rechtman, *Aperiodicity at the boundary of chaos*, to appear at Ergodic Theory and Dynamical Systems.

[P10] S. Hurder and A. Rechtman, *Perspectives on Kuperberg flows*, to appear at the proceedings of the 31st Summer Conference on Topology and its Applications.

[Kat73] A. Katok, *Ergodic perturbations of degenerate integrable Hamiltonian systems*, Math. USSR Izv., 7, 535, 1973.

[Kat80] A. Katok, *Lyapunov exponents, entropy and periodic orbits for diffeomorphisms*, Inst. Hautes Études Sci. Publ. Math., 51, 137–173, 1980.

[KT97] A. Katok and J.-P. Thouvenot, *Slow entropy type invariants and smooth realization of commuting measure-preserving transformations*, Ann. Inst. H. Poincaré Probab. Statist., 33, 323–338, 1997.

[Kni81] R. J. Knill, *A C^∞ flow on $\mathbb{S}^3$ with a Denjoy minimal set*, J. Differential Geom., 16, no. 2, 271 – 280, 1981.

[Kud14] E. A. Kudryavtseva, *Conjugation invariants on the group of area-preserving diffeomorphisms of the disk*, Math. Notes, 95, 877–880, 2014.

[Kud16] E. A. Kudryavtseva, *Helicity is the only invariant of incompressible flows whose derivative is continuous in C^1-topology*, Math. Notes, 99, 611–615, 2016.

[Kup96] G. Kuperberg, *A volume-preserving counterexample to the Seifert conjecture*, Comment. Math. Helv., 71, 70–97, 1996.

[Kup94] K. Kuperberg, *A smooth counterexample to the Seifert conjecture*, Ann. of Math. (2), 140, 723–732, 1994.

[KK96] G. Kuperberg and K. Kuperberg, *Generalized counterexamples to the Seifert conjecture*, Ann. of Math. (2), 144, 239–268, 1996.

[MS82] S. Mardešić and J. Segal, Shape theory: The inverse system approach, North-Holland Math. Library, Vol. 26, North-Holland Publishing Co., Amsterdam, 1982.

[Mat95] S. Matsumoto, *Kuperberg's C^∞ counterexample to the Seifert conjecture*, Sūgaku, Mathematical Society of Japan, 47, 38–45, 1995. Translation: Sugaku Expositions, 11, 39–49, 1998, Amer. Math. Soc.

[Mof69] K. Moffatt *The degree of knottedness of tangle vortex lines*, J. Fluid. Mech., 106, 117–129, 1969.

[Mor61] J.-J. Moreau, *Constantes d'un îlot tourbillonnaire en fluide parfait barotrope*, C. R. Acad. Sci. Paris, 252, 2810–2812, 1961.

[Mor00] F. Morgan, Geometric measure theory. A beginner's guide, Third edition, Academic Press, Inc., San Diego, CA, 2000.

[Ozw10] M. Ozawa, *Waist and trunk of knots*, Geom. Dedicata, 149, 85–94, 2010.

[PW77] P.B. Percell and F.W. Wilson, Jr., *Plugging flows*, Trans. Amer. Math. Soc., 233, 93–103, 1977.

[Sch74] P.A. Schweitzer, *Counterexamples to the Seifert conjecture and opening closed leaves of foliations*, Ann. of Math. (2), 100, 386–400, 1974.

[Sei1950] H. Seifert, *Closed integral curves in* 3*-space and isotopic two-dimensional deformations*, Proc. Amer. Math. Soc., 1, 287–302, 1950.

[Tait1877] P. Tait, *On knots*, Trans. Roy. Soc. Edin., 28, 145–190, 1877.

[Tau09] C. H. Taubes, *An observation concerning uniquely ergodic vector fields on 3-manifolds*, J. Gökova Geom. Topol. GGT 3, 9 –21, 2009.

[Tho73] E.S. Thomas, Jr. *One-dimensional minimal sets*, Topology, 12, 233–242, 1973.

[Tho1867] W. Thomson, *On Vortex Atoms*, Proc. Roy. Soc. Edinburgh, 6, 94–105, 1867; reprinted in Phil. Mag., 34, 15–24, 1867.

[Vog02] T. Vogel, *On the asymptotic linking number*, Proc. Amer. Math. Soc., 131, 2289–2297, 2002.

[Wil66] F.W. Wilson, Jr., *On the minimal sets of non-singular vector fields*, Ann. of Math. (2), 84, 529–536, 1966.

[Wol58] L. Woltjer, *A Theorem on Force-free magnetic Fields*, Proc. Natl. Acad. Sci. USA, 44, 489–491, 1958.

[Zup12] A. Zupan, *A lower bound on the width of satellite knots*, Topology Proc., 40, 179–188, 2012.